TROISIÈME CYCLE DE LA PHYSIQUE

EN SUISSE ROMANDE

MATHEMATICAL DIFFRACTION THEORY IN EUCLIDIAN SPACES

Michael BAAKE

Fakultät für Mathematik, Universität Bielefeld
D – 33501 Bielefeld

Hôte du
Laboratoire de Cristallographie
EPFL Lausanne

SEMESTRE D'HIVER 2004-2005

TROISIÈME CYCLE DE LA PHYSIQUE

EN SUISSE ROMANDE

UNIVERSITÉS

DE

FRIBOURG - GENÈVE - NEUCHÂTEL

&

ÉCOLE POLYTECHNIQUE FÉDÉRALE DE LAUSANNE

****

MATHEMATICAL DIFFRACTION THEORY IN EUCLIDEAN SPACES: AN INTRODUCTORY SURVEY

MICHAEL BAAKE

Abstract. Mathematical diffraction theory is concerned with the Fourier transform of the autocorrelation of translation bounded complex measures. While the latter are meant to encapsulate the relevant order of various forms of matter, the corresponding diffraction measures describe the outcome of kinematic diffraction experiments, as obtained from X-ray or neutron scattering in the far field (or Fraunhofer) picture.

In this introductory article, the mathematical approach to diffraction is summarized, with special emphasis on simple derivations of results. Apart from (fully) periodic order, also aperiodic order is discussed, both in terms of model sets (perfect order) and various stochastic extensions (lattice gases and random tilings).

Keywords: Diffraction Theory, Lattice Systems, Quasicrystals, Disorder

Introduction

The diffraction theory of crystals is a subject with a long history, and one can safely say that it is well understood [31, 21]. Even though the advent of quasicrystals, with their sharp diffraction images with perfect non-crystallographic symmetry, seemed to question the general understanding, the diffraction theory of perfect quasicrystals, in terms of the cut and project method, is also rather well understood by now, see [36, 37] and references therein. It should be noted though that this extension was by no means automatic, and required a good deal of mathematics to clear up the thicket. More recently, this has found an extension to the general setting of locally compact Abelian groups [63, 64], which can be seen as a natural frame for mathematical diffraction theory and covers quite a number of interesting new cases [14].

Another area with a wealth of knowledge is the diffraction theory of imperfect crystals and amorphous bodies [31, 70], but the state of affairs here is a lot less rigorous, and many results and features seem to be more or less folklore. For example, the diffraction of stochastic systems, as soon as they are not bound to a lattice, is only in its infancy, see [11, 38, 48] for some recent addition to its rigorous treatment. This does not mean that one would not know what to expect. In fact, one can often find a qualitative argument in

the literature, but no proof. May this be acceptable from a practical angle, it seems rather unsatisfactory from a more fundamental point of view. In other words, the answer to the question which distributions of matter diffract is still incomplete, and certainly less obvious than one would like to believe, compare the discussion in [36, Sec. 6] and also [62, 69].

Note that this question contains several different aspects. On the one hand, one would like to know, in rigorous terms, which circumstances imply the diffraction image to be well defined in the sense that it has a unique infinite volume limit. This is certainly the case if one can refer to the ergodicity of the underlying distribution of scatterers [24, 36, 64], in particular, if their positional arrangement is linearly repetitive [49]. However, such uniqueness is often difficult to assess, or actually violated, in situations *without* underlying ergodicity properties, see [13] for an example. On the other hand, even if the image is uniquely defined (perhaps after suitable restrictions to the way the limit is taken), one still wants to know whether it contains Bragg peaks or not, or whether there is any diffuse scattering present in it.

This situation certainly did not improve with the more detailed investigation of quasicrystals, e.g., their less perfect versions, and in particular with the study of the so-called random tilings [26, 32, 57]. Again, there is a good deal of folklore available, and a careful reasoning based upon scaling arguments (compare [41, 32]) seems to give convincing and rather consistent results on their diffraction properties. However, various details, and in particular the exact nature of the diffraction measure, have always been the topic of ongoing discussion, so that a more rigorous treatment is desirable. It is the aim of this summary to introduce a general setting that allows for the systematic development of a rigorous mathematical theory of diffraction, both of perfect and of random structures.

Let us summarize how this survey is organized. We start with a recapitulation of the measure theoretic setup needed for mathematical diffraction theory, where we essentially follow Hof [36, 37], but adapt and extend it to our needs. We shall be a little bit more explicit here than needed for an audience with background in mathematics or mathematical physics, because we hope that the article becomes more self-contained that way, and hence more readable for physicists and crystallographers who usually do not approach problems of diffraction theory in these more rigorous terms. We consider this as part of an attempt to penetrate the communication barrier.

Our first step, after introducing translation bounded measures in a summary with suitable references, including a brief discussion of spectral types and their relation to well-known concepts in crystallography, we shall exploit the so-called Poisson summation formula. This powerful result is at the heart of the general diffraction formula for periodic systems, and should be helpful to understand them from this more abstract point of view. The natural next step then consists in an extension to the diffraction of lattice subsets (including weighted versions), and an illustrative result on homometric structures.

This is followed by a brief recapitulation of the diffraction theory of model sets, before we continue with a more detailed discussion of lattice systems with disorder. Our main interest here is the spectral structure of lattice gases with short range interaction, such as that based upon the classical ferromagnetic Ising model. A common feature of many of these models is that they do not create any singular continuous component in the diffraction image.

Finally, we present a short summary of the present situation for the diffraction of random tilings, with explicit results for the case of one dimension. In the plane, rigorous results are known for cases that derive from exactly solved models of statistical mechanics, such as certain dimer models, while the genuinely non-crystallographic cases are only understood on a heuristic level at present – meaning that there are well supported conjectures, but no proofs.

Mathematical recollections

Diffraction problems have many facets, but one important question certainly is which distributions of atoms lead to well-defined diffraction images, and if so, to what kind of images. This is a difficult problem, far from being solved. So, one often starts, as we shall also do here, by looking at "diffraction at infinity" from single-scattering, where it essentially reduces to questions of Fourier analysis [2, Sec. 6]. This is also called *kinematic diffraction* in the Fraunhofer picture [21], and we are looking into the more mathematical aspects of that now. Mathematical diffraction theory, in turn, is concerned with spectral properties of the Fourier transform of the autocorrelation measure of unbounded (but usually translation bounded, see below) complex measures. Let us therefore first introduce and discuss the notions involved. Here, we start from the presentation in [36, 37] where the linear functional approach to measures is taken, compare [23] for details and background material. We also introduce our notation this way.

0.1. **Measures.** For simplicity, we shall introduce measures as linear functionals, and then connect them to the standard approach via σ-algebras of measurable sets by means of the Riesz-Markov representation theorem, see [17, 18, 56] for background material.

Let $\mathcal{K} = \mathcal{K}(\mathbb{R}^n)$ be the space of complex-valued continuous functions with compact support. A (complex) *measure* μ on $\mathbb{R}^n$ is a linear functional on $\mathcal{K}$ with the extra condition that for every compact set $K \subset \mathbb{R}^n$ there is a constant a_K such that

$$|\mu(g)| \le a_K \, \|g\|_\infty \tag{1}$$

for all $g \in \mathcal{K}$ with support in K; here, $\|g\|_\infty := \sup_{x\in K} |g(x)|$ is the supremum norm of g. If μ is a measure, the *conjugate* of μ is defined by the mapping $g \mapsto \overline{\mu(\bar{g})}$. It is again a measure and denoted by $\bar{\mu}$. A measure μ is called *real* (or signed), if $\bar{\mu} = \mu$, or, equivalently, if $\mu(g)$ is real for all real-valued $g \in \mathcal{K}$. A measure μ is called *positive* if $\mu(g) \ge 0$ for all

$g \geq 0$. For every measure μ, there is a smallest positive measure, denoted by $|\mu|$, such that $|\mu(g)| \leq |\mu|(g)$ for all non-negative $g \in \mathcal{K}$, and this is called the *total variation* (or absolute value) of μ.

A measure μ is *bounded* (or finite) if $|\mu|(\mathbb{R}^n)$ is finite (with obvious meaning, see below), otherwise it is called unbounded. Note that a measure μ is continuous on $\mathcal{K}$ with respect to the topology induced by the norm $\|.\|_\infty$ if and only if it is bounded [23, Ch. XIII.20]. In view of this, the vector space of measures on $\mathbb{R}^n$, $\mathcal{M}(\mathbb{R}^n)$, is given the *vague topology*, i.e., a sequence of measures $\{\mu_n\}$ converges vaguely to μ if $\lim_{n\to\infty} \mu_n(f) = \mu(f)$ in $\mathbb{C}$ for all $f \in \mathcal{K}$. This is just the weak-* topology on $\mathcal{M}(\mathbb{R}^n)$, in which all the "standard" linear operations on measures are continuous, compare [56, p. 114] for some consequences of this. The measures defined this way are, by proper decomposition [23, Ch. XIII.2 and Ch. XIII.3] and an application of the Riesz-Markov representation theorem, see [56, Thm. IV.18] or [18, Thm. 69.1], in one-to-one correspondence with the regular Borel measures on $\mathbb{R}^n$, wherefore we identify them. The σ-algebra of measurable sets is formed by the Borel sets, i.e., the smallest σ-algebra that contains all open (and hence also all closed) subsets of $\mathbb{R}^n$, in its standard topology, see [56] for details. In particular, we write $\mu(A)$ (measure of a set) and $\mu(f)$ (measure of a function) for simplicity.

The space of complex measures is much too general for our aims, and we have to restrict ourselves to a natural class of objects now. A measure μ is called *translation bounded* [1] if for every compact set $K \subset \mathbb{R}^n$ there is a constant b_K such that

$$\sup_{x\in\mathbb{R}^n} |\mu|(K+x) \;\leq\; b_K \,. \tag{2}$$

For example, if $\varLambda$ is a point set of *finite local complexity*, i.e., if the set $\Delta = \varLambda - \varLambda$ of differences is discrete and closed, the weighted Dirac comb

$$\omega_{\varLambda} \;:=\; \sum_{x\in\varLambda} w(x)\, \delta_x \,, \tag{3}$$

where δ_x is Dirac's measure at point x, is certainly translation bounded if the $w(x)$ are complex numbers with $\sup_{x\in\varLambda} |w(x)| < \infty$. This is so because Δ discrete and closed implies that $0 \in \Delta$ is isolated and the points of $\varLambda$ are separated by a minimal distance, hence $\varLambda$ is uniformly discrete. Note that such a restriction is neither necessary, nor even desirable (it would exclude the treatment of gases and liquids), but it is fulfilled in all our examples below and puts us into a good setting in all cases where we cannot directly refer to pointwise ergodic theorems.

0.2. **Autocorrelations.** For any (continuous) function g, define $\tilde{g}$ by $\tilde{g}(x) := \overline{g(-x)}$. This is properly extended to measures via $\tilde{\mu}(g) := \overline{\mu(\tilde{g})}$. If f and g are in $\mathcal{K}$, one can define their *convolution* via

$$\bigl(f * g\bigr)(x) \;:=\; \int_{\mathbb{R}^n} f(x-y)\, g(y)\, \mathrm{d}y \,, \tag{4}$$

which can be extended to the case that one function is bounded while the other is integrable. Of particular interest is the function $g * \tilde{g}$, with g integrable, which can be written as

$$\bigl(g * \tilde{g}\bigr)(x) \;=\; \int_{\mathbb{R}^n} g(x+z)\,\overline{g(z)}\,\mathrm{d}z \;=\; \int_{\mathbb{R}^n} g(w)\,\overline{g(w-x)}\,\mathrm{d}w\,. \tag{5}$$

Sometimes, the rather convenient notation $g\tilde{*}g$ is used for this "folded-over" variant of a convolution [25].

Recall that the convolution $\mu * \nu$ of two measures μ and ν is again a measure, given by

$$\bigl(\mu * \nu\bigr)(g) \;:=\; \int_{\mathbb{R}^n \times \mathbb{R}^n} g(x+y)\,\mathrm{d}\mu(x)\,\mathrm{d}\nu(y)\,, \tag{6}$$

which is well-defined if at least one of the two measures has compact support, or is a finite measure, while the other is translation bounded. For $R > 0$, let $B_R = B_R(0)$ denote the closed ball of radius R with centre 0, and $\mathrm{vol}(B_R)$ its volume. The characteristic function of a set $A \subset \mathbb{R}^n$ is denoted by 1_A. Let μ_R be the restriction of a measure μ to the ball B_R. Since μ_R then has compact support,

$$\gamma^R \;:=\; \frac{1}{\mathrm{vol}(B_R)}\,\mu_R * \widetilde{\mu_R} \tag{7}$$

is well defined. Every vague point of accumulation of γ^R, as $R \to \infty$, is called an *autocorrelation* of μ, and as such it is, by definition, a measure. If only one point of accumulation exists, the autocorrelation is unique, and it is called the *natural autocorrelation*. It will be denoted by γ or by γ_μ to stress the dependence on μ. One way to establish the existence of the limit is through the pointwise ergodic theorem, compare [24], if such methods apply. If not, explicit convergence proofs will be needed, as is apparent from known examples [13] and counterexamples [49].

Translation bounded measures μ have the property that all γ^R are uniformly translation bounded, and $\{\gamma^R \mid R > 0\}$ is precompact in the vague topology. If the natural autocorrelation exists, it is clearly also translation bounded [36, Prop. 2.2]. This is a very important property, upon which a fair bit of our later analysis rests. If the limit does not exist, there is still at least one converging subsequence. Each such subsequence converges toward *an* autocorrelation, each of which is then translation bounded and positive definite.

Let us mention, at this point, that different measures can lead to the same natural autocorrelation, namely if one adds to a given measure μ a sufficiently "meager" measure ν, see [36, Prop. 2.3] for details. In particular, adding or removing finitely many points from $\varLambda$, or points of density 0, does not change γ, if it exists.

Note that Hof [36] uses cubes rather than balls in his definition of γ^R. This simplifies some of his proofs technically, but they also work for balls which are more natural objects in a physical context. This is actually not important for our purposes here. One should keep in mind, however, that the autocorrelation will, in general, depend on the shape of the volume over which the average is taken — with obvious meaning for the experimental

situation where the shape corresponds to the aperture. To get rid of this problem, one often restricts the class of models to be considered and defines the limits along arbitrary van Hove sequences, thus demanding a stricter version of uniqueness [61, Sec. 2.1].

Let us focus on the Dirac comb $\omega = \omega_{\varLambda}$ from (3), with $\varLambda$ a point set of finite local complexity, and let us assume for the moment that its natural autocorrelation γ_{ω} exists and is unique (Lagarias and Pleasants construct an example where this fails [49]). A short calculation shows that $\widetilde{\omega_{\varLambda}} = \sum_{x\in\varLambda} \overline{w(x)}\, \delta_{-x}$. Since $\delta_x * \delta_y = \delta_{x+y}$, we get

$$\gamma_{\omega} \;=\; \sum_{z\in\Delta} \eta(z)\delta_z \,, \tag{8}$$

where the autocorrelation coefficient $\eta(z)$, for $z \in \Delta$, is given by the limit

$$\eta(z) \;=\; \lim_{R\to\infty} \frac{1}{\mathrm{vol}(B_R)} \sum_{\substack{x\in\varLambda_R \\ x-z\in\varLambda}} w(x)\, \overline{w(x-z)} \,, \tag{9}$$

with $\varLambda_R := \varLambda \cap B_R$. Eq. (9) actually uses the fact that $\{B_R \mid R > 0\}$ has the van Hove property. In this case, it basically means that the surface to bulk ratio of a sphere of radius R goes to 0 as $R \to \infty$.

Conversely, if the limits in (9) exist for all $z \in \Delta$, the natural autocorrelation exists, too, because Δ is discrete and closed by assumption, and (8) thus uniquely defines a translation bounded measure of positive type. This is one advantage of using sets of finite local complexity.

0.3. **Fourier transform and distributions.** We now have to turn our attention to the Fourier transform of unbounded measures on $\mathbb{R}^n$ which ties the previous together with the theory of tempered distributions [65], see [1, 64] for extensions to other locally compact Abelian groups.

Let $\mathcal{S}(\mathbb{R}^n)$ be the space of rapidly decreasing C^∞ functions [65, Ch. VII.3], also called Schwartz functions. This space certainly contains all C^∞-functions with compact support, but also functions such as $P(x)\exp(-x^2)$, where P is an arbitrary polynomial in $x = (x_1, \ldots, x_n)$. By the Fourier transform of a Schwartz function $\phi \in \mathcal{S}(\mathbb{R}^n)$, we mean

$$(\mathcal{F}\phi)(k) \;=\; \widehat{\phi}(k) \;:=\; \int_{\mathbb{R}^n} e^{-2\pi i k\cdot x}\, \phi(x)\, \mathrm{d}x \,, \tag{10}$$

which is again a Schwartz function [65, 56]. Here, $k \cdot x$ is the Euclidean inner product of $\mathbb{R}^n$, simply written kx from now on. The inverse operation exists and is given by

$$(\mathcal{F}^{-1}\psi)(x) \;=\; \check{\psi}(x) \;=\; \int_{\mathbb{R}^n} e^{2\pi i x k}\, \psi(k)\, \mathrm{d}k \,. \tag{11}$$

The Fourier transform $\mathcal{F}$ is a linear bijection from $\mathcal{S}(\mathbb{R}^n)$ onto itself, and is bi-continuous [56, Thm. IX.1]. Our definition (with the factor 2π in the exponent) results in the usual

properties, such as

$$\check{\check{\phi}} \;=\; \phi \qquad \text{and} \qquad \widehat{\widehat{\psi}} = \psi \,.$$

The convolution theorem takes the simple form $(\phi_1 * \phi_2)\widehat{\ } = \widehat{\phi}_1 \cdot \widehat{\phi}_2$, where the convolution of two Schwartz functions is given by formula (4). Let us also mention that $\mathcal{F}$ has a unique extension to the Hilbert space $L^2(\mathbb{R}^n)$, often called the Fourier-Plancherel transform, which turns out to be a unitary operator of fourth order, i.e., $\mathcal{F}^4 = \mathrm{Id}$. This is so because $(\mathcal{F}^2\phi)(x) = \phi(-x)$, see [60] for details.

A *tempered distribution* is a continuous linear functional on Schwartz space $\mathcal{S}(\mathbb{R}^n)$. The tempered distributions thus form the dual space, denoted by $\mathcal{S}'(\mathbb{R}^n)$. In line with the general literature, we shall use the notation $(T, \phi) := T(\phi)$ for the evaluation of $T \in \mathcal{S}'(\mathbb{R}^n)$ with a function $\phi \in \mathcal{S}(\mathbb{R}^n)$.

Finally, the matching definition of the Fourier transform of a tempered distribution [65] $T \in \mathcal{S}'(\mathbb{R}^n)$ is

$$\widehat{T}(\phi) \;:=\; T(\widehat{\phi}) \tag{12}$$

for all Schwartz functions ϕ, as usual. The Fourier transform is then a linear bijection of $\mathcal{S}'(\mathbb{R}^n)$ onto itself which is the unique weakly continuous extension of the Fourier transform on $\mathcal{S}(\mathbb{R}^n)$ [56, Thm. IX.2]. This is important, because it means that weak convergence of a sequence of tempered distributions, $T_n \to T$ as $n \to \infty$, implies weak convergence of their Fourier transforms, i.e., $\widehat{T}_n \to \widehat{T}$.

0.4. **Examples.** Let us give three examples here, which will reappear later. First, the Fourier transform of Dirac's measure δ_x at x is given by

$$\widehat{\delta_x} \;=\; e^{-2\pi i x y} \tag{13}$$

where the right hand side is actually the Radon-Nikodym density, and hence a function of the variable y, that represents the corresponding measure (we shall not distinguish an absolutely continuous measure from its density, if misunderstandings are unlikely).

Second, consider the Dirac comb $\delta_{\varGamma} = \sum_{x \in \varGamma} \delta_x$ of a lattice $\varGamma \subset \mathbb{R}^n$ (i.e., a discrete subgroup of $\mathbb{R}^n$ such that the factor group $\mathbb{R}^n/\varGamma$ is compact). Then, one has

$$\widehat{\delta_{\varGamma}} \;=\; \mathrm{dens}(\varGamma) \cdot \delta_{\varGamma^*} \,, \tag{14}$$

where $\mathrm{dens}(\varGamma)$ is the density of $\varGamma$, i.e., the number of lattice points per unit volume, and $\varGamma^*$ is the *dual* (or reciprocal) lattice,

$$\varGamma^* \;:=\; \{y \in \mathbb{R}^n \mid xy \in \mathbb{Z} \text{ for all } x \in \varGamma\} \,. \tag{15}$$

Equation (14) is *Poisson's summation formula* for distributions [65, p. 254] and will be central for the determination of the Bragg part of the diffraction measure. Finally, putting

these two pieces together, we also get the formula

$$\sum_{k\in\varGamma} e^{-2\pi ikx} \;=\; \mathrm{dens}(\varGamma)\cdot \sum_{y\in\varGamma^*} \delta_y \,, \tag{16}$$

to be understood in the distribution sense. We shall derive Equations (14) and (16) in detail below.

0.5. **Measures and distributions.** Though both are defined as linear functionals, there is an important difference between measures and tempered distributions. While the former are defined on continuous functions of compact support, the latter need Schwartz functions as arguments. In particular, measures need not be tempered distributions at the same time, e.g., if they grow too fast when moving to ∞. If a measure μ also defines a tempered distribution T_μ, via $T_\mu(\phi) = \mu(\phi)$ for all $\phi \in \mathcal{S}(\mathbb{R}^n)$, the measure is called a *tempered measure*. A sufficient condition for a measure to be tempered is that it increases only slowly, in the sense that $\int (1+|x|)^{-\ell}\,\mathrm{d}|\mu|(x) < \infty$ for some $\ell \in \mathbb{N}$, see [65, Thm. VII.VII]. Consequently, every translation bounded measure is tempered – and such measures form the right class for our purposes. So, this does not cause much of a problem in our present setting.

Conversely, a tempered distribution need not define a measure, and this is indeed a problem in the systematic development of mathematical diffraction theory in general, compare [36]. To make this concrete, consider the distribution δ_x' defined by $\delta_x'(\phi) := -\phi'(x)$, where the symbol $'$ denotes the derivative with respect to x. This is unambiguous because ϕ is C^∞, and tempered distributions (also called generalized functions) provide a minimal scheme where all "functions" are automatically infinitely differentiable – in this distribution sense. However, δ_x' does *not* define a measure, because one cannot give $\delta_x'(g)$ a clear meaning for continuous functions g of compact support – just think of an example that is not differentiable at x. This kind of problem must be avoided.

Nevertheless, if we start from a tempered measure, we shall usually not distinguish between the measure and the corresponding distribution, i.e., we shall write $\widehat{\mu}$ for $\widehat{T_\mu}$. The Fourier transform of a tempered measure is a tempered distribution, but it need *not* be a measure. However, if μ is of *positive type* (also called positive definite) in the sense that $\mu(\phi * \tilde{\phi}) \geq 0$ for all $\phi \in \mathcal{S}(\mathbb{R}^n)$, then $\widehat{\mu}$ is a positive measure by the Bochner-Schwartz Theorem [56, Thm. IX.10]. Every autocorrelation γ is, by construction, a measure of positive type, so that $\widehat{\gamma}$ is a positive measure. This explains why this is a natural approach to kinematic diffraction, because the observed intensity pattern is represented by a positive measure that tells us which amount of intensity is present in a given volume.

0.6. **Decomposition of measures.** Also, taking Lebesgue's measure as a reference, (positive) measures μ permit a unique decomposition into three parts,

$$\mu \;=\; \mu_{\mathrm{pp}} + \mu_{\mathrm{sc}} + \mu_{\mathrm{ac}} \,, \tag{17}$$

where 'pp', 'sc' and 'ac' stand for pure point, singular continuous and absolutely continuous, see [56, Sec. I.4] for background material. The set $P = \{x \mid \mu(\{x\}) \neq 0\}$ is called the set of pure points of μ, which supports the so-called Bragg part μ_{pp} of μ. Note that P is at most a countable set. What remains, i.e., $\mu - \mu_{\mathrm{pp}}$, is the "continuous background" of μ, and this is the unambiguous and mathematically precise formulation of what such terms are supposed to mean. Depending on the context, one also writes

$$\mu \;=\; \mu_{\mathrm{pp}} + \mu_{\mathrm{cont}} \;=\; \mu_{\mathrm{sing}} + \mu_{\mathrm{ac}}\,, \tag{18}$$

where $\mu_{\mathrm{cont}} = \mu_{\mathrm{sc}} + \mu_{\mathrm{ac}} = \mu - \mu_{\mathrm{pp}}$ is the continuous part of μ (see above) and $\mu_{\mathrm{sing}} = \mu_{\mathrm{pp}} + \mu_{\mathrm{sc}}$ is the singular part, i.e., $\mu_{\mathrm{sing}}(R) = 0$ for some set R whose complement $S = \mathbb{R}^n \setminus R$ has vanishing Lebesgue measure (in other words, μ_{sing} is concentrated to S, a set of vanishing Lebesgue measure, in the sense that $\mu_{\mathrm{sing}} = \mu_{\mathrm{sing}}|_S$). Finally, the absolutely continuous part, which is usually called diffuse[1] scattering [40] in crystallography, can be represented by its Radon-Nikodym density [56, Thm. I.19] which is often very handy. Examples for the various spectral types can easily be constructed by different substitution systems, see [55] and references therein for details.

It is possible to construct a simple example in the context of stochastic product tilings where all three spectral types are present, see [7, 34] for details, though their meaning will need a careful discussion. In particular, a measure that is concentrated to a line or a circle in the plane is singular, but this is not the 'generic' case of a singular continuous measure here (because it can be written as a product measure, at least locally). More generally, one can have a measure that is concentrated to an uncountable set of points in a region (or the entire plane) that is 'scattered around' (or even dense) and, at the same time, still of measure 0. Another example of interest in this context is Danzer's aperiodic tiling that is built from a single proto-tile [22]. It can be shown to have singular diffraction [5].

Hof discusses a number of properties of Fourier transforms of tempered measures [36, 37]. Important to us is the observation that temperedness of μ together with positivity of $\widehat{\mu}$ implies translation boundedness of $\widehat{\mu}$ [36, Prop. 3.3]. So, if μ is a translation bounded measure whose natural autocorrelation γ_μ exists, then γ_μ is also translation bounded (see above), hence tempered, and thus the positive measure $\widehat{\gamma}_\mu$ is both translation bounded and tempered, too. For a more general discussion of translation bounded measures and their Fourier transforms, also in connection with almost periodicity, we refer to [30].

In what follows, we shall mainly restrict ourselves to the spectral analysis of measures μ that are concentrated on uniformly discrete point sets. They are seen as an idealization of pointlike scatterers at uniformly discrete positions, in the infinite volume limit. The rationale behind this is as follows. If one understands these cases well, one can always

[1] In fact, the precise meaning of diffuse scattering, compare [40, 31], varies with the context, and can also contain some singular continuous component. We prefer to reserve it for the absolutely continuous part, as the sc part already shows some form of coherence.

extend both to measures with extended local profiles (e.g., by convolution with a smooth function of compact support or with a Schwartz function) and to measures that describe diffraction at positive temperatures (e.g., by using Hof's probabilistic treatment [38], which was recently extended to more general settings by Külske [48]). The treatment of gases or liquids might need some additional tools, but we focus on situations that stem from solids with long-range order and different types of structural disorder, because we feel that this is where the biggest and most urgent gaps in our understanding are at present.

1. Poisson's summation formula (PSF)

There is a very simple, and yet completely rigorous, approach to the diffraction formula of a fully periodic measure. It is based on Poisson's summation formula (PSF). Though this is one of the really central identities in mathematics, it is relatively unknown in the applied sciences. Therefore, I take the opportunity to introduce it in some details, followed by some applications.

1.1. **PSF for functions.** A (continuous) function $g\colon \mathbb{R}^n \longrightarrow \mathbb{C}$ is called $\mathbb{Z}^n$-*periodic*, if $g(x+k) = g(x)$ for all $x \in \mathbb{R}^n$ and all $k \in \mathbb{Z}^n$. Let $\mathbb{T}^n := \mathbb{R}^n/\mathbb{Z}^n$ denote the n-dimensional torus (identified with a fundamental domain of the lattice $\mathbb{Z}^n$, e.g., with $[0,1)^n$), and define the Fourier series coefficients

$$c_k \;=\; \int_{\mathbb{T}^n} e^{-2\pi i k x} g(x)\,\mathrm{d}x \;=\; \int_0^1 e^{-2\pi i k_n x_n} \ldots \int_0^1 e^{-2\pi i k_1 x_1}\, g(x)\,\mathrm{d}x_1 \ldots \mathrm{d}x_n \tag{19}$$

for $k \in \mathbb{Z}^n$, with $x = (x_1, \ldots, x_n)$. Let us further assume that g is infinitely differentiable, i.e., that $g \in C^\infty(\mathbb{R}^n)$. This is a sufficient condition for the *Fourier series*

$$g(x) \;=\; \sum_{k\in\mathbb{Z}^n} c_k\, e^{2\pi i k x} \tag{20}$$

to converge uniformly towards g. To see this, one considers d-fold partial integration (with $d \in \mathbb{N}$) in (19), in the direction of the maximal k-component. This produces prefactors of the form $1/k_\ell^d$ in front of the integral. As all derivatives that occur in this process are uniformly bounded, there is a constant $C = C(d,g)$ such that

$$|c_k| \;\leq\; \frac{C}{\|k\|_\infty^d}\,.$$

With $d > n$, one obtains, by standard arguments from calculus, the absolute and uniform convergence of the Fourier series.

Consider now a Schwartz function $\phi \in \mathcal{S}(\mathbb{R}^n)$, with its Fourier transform $\widehat{\phi}(k) = \int_{\mathbb{R}^n} e^{-2\pi i k x}\phi(x)\,\mathrm{d}x$ as defined above.

Proposition 1 (PSF for functions)**.** *If $\phi \in \mathcal{S}(\mathbb{R}^n)$, one has $\sum_{m\in\mathbb{Z}^n} \phi(m) = \sum_{m\in\mathbb{Z}^n} \widehat{\phi}(m)$.*

Proof. Define $g(x) = \sum_{\ell\in\mathbb{Z}^n} \phi(x+\ell)$. Due to $\phi \in \mathcal{S}(\mathbb{R}^n)$, this is a uniformly convergent sum. Also, g is both infinitely differentiable and $\mathbb{Z}^n$-periodic. If c_m is the Fourier coefficient as defined in (19), we have, from (20),

$$\sum_{m\in\mathbb{Z}^n} c_m \;=\; g(0) \;=\; \sum_{m\in\mathbb{Z}^n} \phi(m)\,.$$

On the other hand, we have

$$\begin{aligned} c_m \;&=\; \int_{\mathbb{T}^n} e^{-2\pi imx} g(x)\,\mathrm{d}x \;=\; \sum_{\ell\in\mathbb{Z}^n} \int_{\mathbb{T}^n} e^{-2\pi imx}\phi(x+\ell)\,\mathrm{d}x \\ &=\; \sum_{\ell\in\mathbb{Z}^n} \int_{\mathbb{T}^n} e^{-2\pi im(x+\ell)}\phi(x+\ell)\,\mathrm{d}x \;=\; \sum_{\ell\in\mathbb{Z}^n} \int_{\ell+\mathbb{T}^n} e^{-2\pi imx}\phi(x)\,\mathrm{d}x \;=\; \widehat{\phi}(m)\,, \end{aligned}$$

where the last step follows from $\mathbb{R}^n = \dot{\bigcup}_{\ell\in\mathbb{Z}^n}(\ell+\mathbb{T}^n)$, with $\dot\cup$ denoting the disjoint union of sets. Since all steps in the calculation are justified by the uniform convergence of our series, the claim follows. □

1.2. **PSF for Dirac combs.** Next, we have to transfer this result to (tempered) measures. To do so, we first formulate it for $\mathbb{Z}^n$-periodic Dirac combs. Recall that the normalized point measure (or Dirac measure) at x is denoted by δ_x and defined by $\delta_x(\phi) := \phi(x)$, for any function ϕ that is continuous at x. In particular, this covers all Schwartz functions. When viewed as a Borel measure (which we are entitled to do by the Riesz-Markov representation theorem mentioned earlier), we have

$$\delta_x(M) \;=\; \begin{cases} 1, & \text{if } x\in M \\ 0, & \text{otherwise} \end{cases}$$

for an arbitrary Borel set $M\subset\mathbb{R}^n$.

If S is a uniformly discrete point set, we define $\delta_S = \sum_{x\in S}\delta_x$, so that one has

$$\delta_S(\phi) \;=\; \sum_{x\in S}\phi(x)$$

for all $\phi\in\mathcal{S}(\mathbb{R}^n)$, where convergence is again a consequence of the properties of ϕ. Let us now consider the set $S=\mathbb{Z}^n$ and its Dirac comb $\delta_{\mathbb{Z}^n}$.

Proposition 2 (PSF for Dirac combs)**.** *In $\mathcal{S}'(\mathbb{R}^n)$, one has the identity $\widehat{\delta_{\mathbb{Z}^n}} = \delta_{\mathbb{Z}^n}$.*

Proof. We have to verify that $(\widehat{\delta_{\mathbb{Z}^n}},\phi) = (\delta_{\mathbb{Z}^n},\phi)$, for all $\phi\in\mathcal{S}(\mathbb{R}^n)$. This is a simple calculation on the basis of Proposition 1:

$$(\widehat{\delta_{\mathbb{Z}^n}},\phi) \;=\; (\delta_{\mathbb{Z}^n},\widehat{\phi}\,) \;=\; \sum_{m\in\mathbb{Z}^n}\widehat{\phi}(m) \;=\; \sum_{m\in\mathbb{Z}^n}\phi(m) \;=\; (\delta_{\mathbb{Z}^n},\phi)$$

which proves the claim. □

At this point, we can come back to the example given in Eq. (16) and explain it for $\varGamma = \mathbb{Z}^n$. Since $(\widehat{\delta_x}, \phi) = (\delta_x, \widehat{\phi}\,) = \widehat{\phi}(x) = \int_{\mathbb{R}^n} e^{-2\pi i x y} \phi(y)\, \mathrm{d}y$, the tempered distribution $\widehat{\delta_x}$ is representable by integration over a (continuous) function. Such distributions are called *regular*, and one uses the short-hand notation $\widehat{\delta_x} = e^{-2\pi i x y}$ for this situation, the right-hand side being the kernel of the integration, written as a function of the variable y. In general, if $g(y)$ is any locally integrable function that does not increase faster than polynomially as $|y| \to \infty$, g defines a tempered T_g distribution via $(T_g, \phi) = \int_{\mathbb{R}^n} g(y) \phi(y)\, \mathrm{d}y$.

Now, with this convention, the following calculation is based on the PSF and obtains a rigorous meaning as an equation in tempered distributions,

$$\sum_{x \in \mathbb{Z}^n} e^{-2\pi i x y} \;=\; \sum_{x \in \mathbb{Z}^n} \widehat{\delta_x} \;=\; \widehat{\delta_{\mathbb{Z}^n}} \;=\; \delta_{\mathbb{Z}^n} \;=\; \sum_{k \in \mathbb{Z}^n} \delta_k \,.$$

Its validity is a direct consequence of Proposition 2.

1.3. **PSF for general lattices.** What remains, is the extension of our setting to general lattices, both for functions and for Dirac combs. If n linearly independent vectors $\{a_1, a_2, \ldots, a_n\}$ in $\mathbb{R}^n$ are given, they span the *lattice*

$$\varGamma \;=\; \mathbb{Z}a_1 \oplus \ldots \oplus \mathbb{Z}a_n \;=\; \{m_1 a_1 + \ldots + m_n a_n \mid m_i \in \mathbb{Z}\} \,.$$

Alternatively, as used above, one can view a lattice $\varGamma$ as a discrete subgroup of $\mathbb{R}^n$ such that $\mathbb{R}^n/\varGamma$ is compact, the latter then being identified with a fundamental domain of $\varGamma$. The dual lattice was already defined in Equation (15).

The lattice can be written as $\varGamma = A\mathbb{Z}^n$, where $A \in \mathrm{GL}(n, \mathbb{R})$ is the invertible matrix that columnwise contains the coordinates of the basis vectors a_m. Observe that, if g is a $\varGamma$-periodic function, $h = g \circ A$ is $\mathbb{Z}^n$-periodic, where $(g \circ A)(x) := g(Ax)$. One now has

$$\sum_{m \in \varGamma} \phi(m) \;=\; \sum_{\ell \in \mathbb{Z}^n} (\phi \circ A)(\ell) \;=\; \sum_{\ell \in \mathbb{Z}^n} \widehat{(\phi \circ A)}(\ell)$$

by means of Proposition 1. A simple calculation shows that $\widehat{(\phi \circ A)}(x) = |\det(A)|^{-1} \widehat{\phi}(Bx)$, where $B = (A^{-1})^t$ is the basis matrix of the dual lattice, i.e., $\varGamma^* = B\mathbb{Z}^n$, and $\mathrm{dens}(\varGamma) := 1/|\det(A)|$ is the density of the lattice $\varGamma$. Putting this together, we can formulate

Theorem 1 (General PSF)**.** *If $\varGamma$ is a lattice in $\mathbb{R}^n$, with dual lattice $\varGamma^*$, and if $\phi \in \mathcal{S}(\mathbb{R}^n)$ is an arbitrary Schwartz function, one has*

$$\sum_{m \in \varGamma} \phi(m) \;=\; \mathrm{dens}(\varGamma) \sum_{\ell \in \varGamma^*} \widehat{\phi}(\ell) \,.$$

Moreover, in $\mathcal{S}'(\mathbb{R}^n)$, one has the following identity of lattice Dirac combs,

$$\widehat{\delta_{\varGamma}} \;=\; \mathrm{dens}(\varGamma)\, \delta_{\varGamma^*} \,.$$

Proof. The first claim follows immediately from the above calculations. To show the identity of the Dirac combs, let ϕ be an arbitrary Schwartz function, and consider

$$\begin{aligned}(\widehat{\delta_{\varGamma}}, \phi) &= (\delta_{\varGamma}, \widehat{\phi}\,) = \sum_{m\in\varGamma} \widehat{\phi}(m) = \operatorname{dens}(\varGamma) \sum_{\ell\in\varGamma^*} \big(\mathcal{F}^2\phi\big)(\ell) \\ &= \operatorname{dens}(\varGamma) \sum_{\ell\in\varGamma^*} \phi(-\ell) = \operatorname{dens}(\varGamma) \sum_{\ell\in\varGamma^*} \phi(\ell) = \operatorname{dens}(\varGamma)\, (\delta_{\varGamma^*}, \phi)\end{aligned}$$

where we have used the general property of the Fourier transform that $\big(\mathcal{F}^2\phi\big)(x) = \phi(-x)$ and the inversion symmetry of lattices. □

1.4. **Lattice periodic measures.** If μ and ν are two (possibly complex) measures on $\mathbb{R}^n$, their *convolution* is defined as in Equation (6), for $g \in \mathcal{K}$, provided the integral exists. In particular, the convolution of any measure with the Dirac measure δ_x is well defined and describes a translation by x.

If $\varGamma$ is a lattice, a measure μ is called *$\varGamma$-periodic* if $\delta_x * \mu = \mu$, for all $x \in \varGamma$. For a function g, one has $(\delta_x * g)(y) = g(x - y)$, which shows the connection to our earlier considerations.

Proposition 3. *If $\varGamma \subset \mathbb{R}^n$ is a lattice, with fundamental domain* $\mathrm{FD}(\varGamma)$*, and if μ is a $\varGamma$-periodic measure on $\mathbb{R}^n$, there is a* finite *measure ϱ supported in* $\mathrm{FD}(\varGamma)$ *so that $\mu = \varrho * \delta_{\varGamma}$.*

Proof. The Voronoi region of $\varGamma$, i.e., the closed set of all points of $\mathbb{R}^n$ whose distance from 0 is not larger than that to any other lattice point, is a (closed) polytope and contains a fundamental domain. By systematically removing part of its boundary (for which there is a standard construction), one can obtain a measurable set B that is a true fundamental domain, i.e., one has $\mathbb{R}^n = \dot{\bigcup}_{t\in\varGamma}(t + B)$, where $\dot{\cup}$ denotes disjoint union.

If we set $\varrho := \mu|_B$, this restriction is a well defined finite measure. One can check that $\mu|_{t+B} = \delta_t * \varrho$, and thus

$$\mu = \sum_{t\in\varGamma} \mu|_{t+B} = \sum_{t\in\varGamma} \delta_t * \varrho = \varrho * \delta_{\varGamma}$$

which establishes the claim. □

This result permits the calculation of the Fourier transform of an arbitrary lattice periodic measure as follows. If μ is $\varGamma$-periodic, we first decompose it as $\mu = \varrho * \delta_{\varGamma}$, according to the last proposition. Then, one simply applies the convolution theorem (this time, the corresponding version for measures resp. tempered distributions):

$$\widehat{\mu} = (\varrho * \delta_{\varGamma})\widehat{\ } = \widehat{\varrho} \cdot \widehat{\delta_{\varGamma}} = \operatorname{dens}(\varGamma)\, \widehat{\varrho}\, \delta_{\varGamma^*}$$

where the last step follows from the general PSF. In particular, $\widehat{\mu}$ is a pure point measure. Note that ϱ has compact support, so $\widehat{\varrho}$ is actually an analytic function which simply defines the amplitudes of the Dirac comb.

1.5. **Application: Diffraction of fully periodic measures.** It is a simple exercise to calculate the autocorrelation of the uniform lattice Dirac comb $\delta_{\varGamma}$, which is $\gamma_{\varGamma} = \mathrm{dens}(\varGamma)\,\delta_{\varGamma}$. Clearly, by another application of the general PSF, one finds

$$\widehat{\gamma_{\varGamma}} \;=\; \bigl(\mathrm{dens}(\varGamma)\bigr)^2\,\delta_{\varGamma^*}\,.$$

In general, a $\varGamma$-periodic (complex) measure ω has the form $\omega = \varrho * \delta_{\varGamma}$ with a finite measure ϱ of compact support, according to Proposition 3. It is not difficult to show that the autocorrelation of ω is then unique, and given by

$$\gamma_{\omega} \;=\; (\varrho * \tilde{\varrho}) * \gamma_{\varGamma} \;=\; \mathrm{dens}(\varGamma)\,(\varrho * \tilde{\varrho}) * \delta_{\varGamma}\,.$$

The diffraction measure, which is the Fourier transform of this, then reads

$$\widehat{\gamma_{\omega}} \;=\; \bigl(\mathrm{dens}(\varGamma)\bigr)^2\,|\widehat{\varrho}\,|^2\,\delta_{\varGamma^*}\,, \tag{21}$$

which is the well-known result for perfect crystals.

Note that the choice of ϱ is not unique – there are, in fact, many possibilities. What finally enters the diffraction formula are the values of $|\widehat{\varrho}\,|^2$ at the points of the dual lattice $\varGamma^*$ only. Also, the same formula applies if ω is given as the convolution $\omega = \varrho * \delta_{\varGamma}$ with an arbitrary *finite* measure ϱ, i.e., with $|\varrho|(\mathbb{R}^n) < \infty$. Let us summarize this as follows.

Theorem 2. *Let $\varGamma$ be a lattice in $\mathbb{R}^n$, and ω a $\varGamma$-invariant measure, given as $\omega = \varrho * \delta_{\varGamma}$ with ϱ a finite measure. Then, the diffraction measure $\widehat{\gamma_{\omega}}$ of ω is given by Equation* (21)*. In particular, $\widehat{\gamma_{\omega}}$ is a pure point measure.* □

An important application of this result is the diffraction of an idealized mono-atomic crystal, where the atomic positions are the points of the lattice $\varGamma$ and ϱ describes the atomic scattering profile. Also, more complicated situations with several types of atoms can be modeled this way, as long as one has a stable density on the unit cell and thus no deviation from periodicity.

2. Diffraction of lattice subsets

As a first step beyond the fully periodic situation, let us look at lattice subsets $S \subset \varGamma$ or, more generally, at weighted lattice Dirac combs

$$\omega \;=\; \sum_{t\in\varGamma} w(t)\,\delta_t \tag{22}$$

with a bounded function $w\colon\, \varGamma \to \mathbb{C}$. Clearly, ω is then a translation bounded measure, and the lattice subset case is contained via the weight function $w(t) = 1_S(t)$, where 1_S is the characteristic function of the set S, i.e., $1_S(t) = 1$ if $t \in S$ and $= 0$ otherwise.

It is clear that such measures ω cannot be fully periodic in general. In fact, generically, they cannot have any period at all. Nevertheless, under rather weak assumptions, the diffraction measure $\widehat{\gamma_{\omega}}$ will be strictly $\varGamma^*$-periodic, independent of its spectral type. It need

not be pure point, but rather of mixed type, the latter situation being generic. This setting includes the large class of *lattice gases*, both with and without (stochastic) interactions.

Let us first sketch the basic idea why this periodicity shows up. Assume that we can find a "nice" continuous function h such that we can rewrite ω of (22) as

$$\omega \;=\; h \cdot \delta_{\varGamma}\,,$$

i.e., h must satisfy $h(t) = w(t)$ for all $t \in \varGamma$. Then, at least on a formal level, one obtains from the convolution theorem, together with the PSF, that

$$\widehat{\omega} \;=\; \widehat{h} * \widehat{\delta_{\varGamma}} \;=\; \bigl(\mathrm{dens}(\varGamma)\,\widehat{h}\bigr) * \delta_{\varGamma^*}\,,$$

which is a $\varGamma^*$-periodic measure – provided all quantities are well defined and all operations justifiable. Unfortunately, this needs some more careful analysis, and it is necessary to do it directly on the level of the autocorrelation rather than on the level of ω itself.

2.1. **Interpolation of the autocorrelation.** Let ω be the weighted Dirac comb from (22), and consider the natural autocorrelation $\gamma_{\omega} = \sum_{z\in\varGamma} \eta(z)\,\delta_z$ with the autocorrelation coefficients

$$\eta(z) \;=\; \lim_{r\to\infty} \frac{1}{\mathrm{vol}(B_r)} \sum_{\substack{t,t'\in\varGamma_r\\ t-t'=z}} w(t)\,\overline{w(t')} \;=\; \lim_{r\to\infty} \frac{1}{\mathrm{vol}(B_r)} \sum_{t\in\varGamma_r} w(t)\,\overline{w(t-z)} \tag{23}$$

where $\varGamma_r = \varGamma \cap B_r(0)$ as before. Note that the last step is correct because the sums, prior to taking the limit, differ only by a surface term that vanishes as $r \to \infty$, see [4] for details.

If we now define $\omega_r = \sum_{t\in\varGamma_r} w(t)\,\delta_t$, we obtain a family $\{\gamma_{\omega_r} \mid r > 0\}$ of finite autocorrelations

$$\gamma_{\omega_r} \;=\; \frac{\omega_r * \widetilde{\omega_r}}{\mathrm{vol}(B_r)}$$

that is, by construction, precompact in the vague topology. Consequently, this family has at least one limit point, i.e., there is a sequence of radii along which the finite autocorrelations converge, towards some γ, say. We shall now look at this specific limit point in detail.

Let ϕ be the C^∞ "hat function"

$$\phi(x) \;:=\; \begin{cases} \exp\bigl(\frac{|x|^2}{|x|^2-1}\bigr), & \text{if } |x| < 1,\\ 0, & \text{otherwise,}\end{cases}$$

and define the smoothing function $h(x) = h_0\,\phi(x/\varepsilon)$ with some $h_0 > 0$ and some $\varepsilon > 0$ that is smaller than half the packing radius of the lattice $\varGamma$. Clearly, one has $\|h\|_\infty = h(0) = h_0 \geq h(x) \geq 0$, and h_0 is now chosen so that

$$\bigl(h * \tilde{h}\bigr)(0) \;=\; \int_{\mathbb{R}^n} h(x)\,\tilde{h}(-x)\,\mathrm{d}x \;=\; \int_{\mathbb{R}^n} |h(x)|^2\,\mathrm{d}x \;=\; \|h\|_2^2 \;=\; 1\,.$$

So, h is now an infinitely smooth bump function that is concentrated to the ball of radius ε centred at 0, with maximum value h_0 at the origin. Such a function is globally *Lipschitz continuous*, i.e., there is a constant L_h such that

$$|h(x) - h(y)| \;\leq\; L_h\, |x-y|$$

for all $x, y \in \mathbb{R}^n$. Moreover, one has

Lemma 1. *If h is an integrable Lipschitz function with global Lipschitz constant L_h, also $\tilde{h}$ and $h * \tilde{h}$ are globally Lipschitz, with $L_{\tilde{h}} = L_h$ and the estimate $L_{h*\tilde{h}} \leq \|h\|_1\, L_h$.*

Proof. The Lipschitz continuity of $\tilde{h}$ with $L_{\tilde{h}} = L_h$ is clear. For the second claim, consider

$$\begin{aligned}\Big|\big(h*\tilde{h}\big)(x) - \big(h*\tilde{h}\big)(y)\Big| \;&=\; \left|\int_{\mathbb{R}^n} h(z)\big(\tilde{h}(x-z) - \tilde{h}(y-z)\big)\,\mathrm{d}z\right| \\ \leq\; \int_{\mathbb{R}^n} |h(z)|\,\big|\tilde{h}(x-z) - \tilde{h}(y-z)\big|\,\mathrm{d}z \;&\leq\; L_h \int_{\mathbb{R}^n} |h(z)|\,|x-y|\,\mathrm{d}z \;\leq\; L_h\,\|h\|_1\,|x-y|\end{aligned}$$

which proves both the Lipschitz property and the estimate. □

Defining $f_r = h * \omega_r$, one finds $f_r(z) = \sum_{t\in\varGamma_r} w(t)\, h(z-t)$ and

$$\big(f_r * \tilde{f}_r\big)(z) \;=\; \sum_{u,v\in\varGamma_r} w(u)\overline{w(v)}\,\big(h*\tilde{h}\big)(z-u-v)\,.$$

Due to the special choice of ε above, one finds that, for $z = t \in \varGamma$, $\big(h*\tilde{h}\big)(t-u-v) = 1$ if and only if $u+v=t$, while it takes the value 0 otherwise. With

$$g_r \;=\; \frac{1}{\mathrm{vol}(B_r)}\,\big(f_r * \tilde{f}_r\big)$$

one can now check that $\lim_{r\to\infty} g_r(t) = \eta(t)$, for all $t \in \varGamma$.

Lemma 2. *The family of functions $\{g_r \mid r > 0\}$ is uniformly Lipschitz, equicontinuous, and uniformly bounded.*

Proof. Define $W = \sup_{t\in\varGamma}|w(t)|$ and observe that $\frac{\mathrm{card}(\varGamma_r)}{\mathrm{vol}(B_r)} = \mathrm{dens}(\varGamma) + \mathcal{O}(\frac{1}{r})$, as $r\to\infty$. Then, it is easy to verify (see [4] for details) that

$$L_{f_r} \;\leq\; \mathrm{card}(\varGamma_r)\, W\, L_h \qquad\text{and}\qquad L_{f_r * \tilde{f}_r} \;\leq\; \mathrm{card}(\varGamma_r)\, W^2\, \|h\|_1\, L_h\,.$$

Transferring this to g_r results in

$$L_{g_r} \;\leq\; \frac{\mathrm{card}(\varGamma_r)}{\mathrm{vol}(B_r)}\, W^2\, \|h\|_1\, L_h + \mathcal{O}(\tfrac{1}{r})\,, \qquad \text{as } r\to\infty,$$

which shows uniform Lipschitz continuity and hence also equicontinuity.

In a similar fashion, one derives

$$|g_r(z)| \;\leq\; \|g_r\|_\infty \;\leq\; \frac{\mathrm{card}(\varGamma_r)}{\mathrm{vol}(B_r)}\, W^2 + \mathcal{O}(\tfrac{1}{r})\,, \qquad \text{as } r\to\infty,$$

from which uniform boundedness follows immediately. □

By Ascoli's theorem, see [50] for an exposition that fits our situation here, we know that $\{g_r \mid r > 0\}$ is relatively compact with respect to $\|.\|_\infty$, so that, on any compact set $K \subset \mathbb{R}^n$, a uniformly converging subsequence is contained with a limit function g that is Lipschitz, positive definite, and satisfies $g(t) = \eta(t)$ for all $t \in \varGamma \cap K$. Since $\mathbb{R}^n$ has a countable base for its topology (a property also called separability), we can extend this to a general function g on all of $\mathbb{R}^n$, with compact convergence of the subsequence. So, we have proved

Proposition 4. *Let $\varGamma$ be a lattice in $\mathbb{R}^n$ and $\omega = \sum_{t\in\varGamma} w(t)\delta_t$ a weighted Dirac comb, with bounded function w. Let γ_ω be any limit point of the family $\{\gamma_{\omega_r} \mid r > 0\}$ of finite autocorrelations. Then, there is a representation of the form*

$$\gamma_\omega \;=\; g \cdot \delta_{\varGamma}$$

with a bounded, positive definite Lipschitz function g. □

2.2. **Diffraction of lattice subsets.** The advantage of the above derivation is that we are now in the situation to start from a well-defined autocorrelation (which can be *any* limit point of the finite autocorrelations, if more than one exists) and to derive its Fourier transform.

Note that the bounded and continuous interpolation function g from Proposition 4 is positive definite, so that, by Bochner's theorem, its Fourier transform $\widehat{g}$ is a *finite* positive measure. So, the following calculation is perfectly justified,

$$\widehat{\gamma_\omega} \;=\; \bigl(g \cdot \delta_{\varGamma}\bigr)\widehat{\ } \;=\; \widehat{g} * \widehat{\delta_{\varGamma}} \;=\; \mathrm{dens}(\varGamma)\, \widehat{g} * \delta_{\varGamma^*}\,,$$

where the convolution theorem was used backwards, followed by another application of the PSF. This gives

Proposition 5. *Under the assumptions of Proposition 4, any diffraction measure $\widehat{\gamma_\omega}$ of the weighted Dirac comb ω is $\varGamma^*$-periodic.* □

Recall that a diffraction measure is always a positive measure. Employing Proposition 3, we may conclude that a finite positive measure ϱ exists that is supported in a fundamental domain and satisfies $\widehat{\gamma_\omega} = \varrho * \delta_{\varGamma^*}$. This is the precise version of the original idea sketched above.

Theorem 3. *Let the assumptions be as in Proposition 4, and let γ_ω be any of the autocorrelations of the weighted Dirac comb ω of (22). Then, the following properties hold.*

(1) *$\gamma_\omega = \varPhi \cdot \delta_{\varGamma}$, with $\varPhi$ an analytic function;*

(2) *$\widehat{\gamma_\omega} = \varrho * \delta_{\varGamma^*}$, with a finite positive measure ϱ of compact support.*

Proof. Most steps have already been derived. That the interpolation function g from above can be replaced by an analytic function Φ, is a simple consequence of the Paley-Wiener theorem, compare [56]. □

Here, we have explicly used the underlying lattice structure. Nevertheless, the type of result is robust in the sense that more general classes of sets, so-called Meyer sets [52], permit a related consideration. In particular, the set of Bragg peak positions is then either relatively dense, or empty, see [67] for details.

2.3. **Complementary lattice subsets.** A particularly interesting situation emerges in the comparison of a lattice subset $S \subset \varGamma$ with its complement $S' = \varGamma \setminus S$. Here, the Dirac combs to be compared are $\omega = \delta_S = \sum_{x\in S} \delta_x$ and $\omega' = \delta_{S'}$. Note that the Dirac comb of (22), when specialized to $w \equiv 1$, results in an autocorrelation with coefficients

$$\eta_S(z) \;=\; \lim_{r\to\infty} \frac{\mathrm{card}\big(S \cap (z+S) \cap B_r(0)\big)}{\mathrm{vol}(B_r(0))} \;=\; \mathrm{dens}\big(S \cap (z+S)\big) \tag{24}$$

for all $z \in \mathbb{R}^n$, provided the limits exist. Otherwise, one restricts to a suitable unbounded sequence of increasing radii, in order to define a fixed accumulation point. This can easily be derived from (23) and the comments following it.

Next, recall that two point sets are called *homometric* if they share the same (natural) autocorrelation. This is an important concept in crystallography, both in theory and practice, because homometric sets cannot be distinguished by (kinematic) diffraction.

Theorem 4. *Let $\varGamma$ be a lattice in $\mathbb{R}^n$, and let $S \subset \varGamma$ be a subset with existing (natural) autocorrelation coefficients $\eta_S(z) = \mathrm{dens}\big(S \cap (z+S)\big)$. Then, the following holds.*

(1) *The autocorrelation coefficients $\eta_{S'}(z)$ of the complement set $S' = \varGamma \setminus S$ also exist. They are $\eta_{S'}(z) = 0$ for all $z \notin \varGamma$ and otherwise, for $z = t \in \varGamma$, satisfy the relation*

$$\eta_{S'}(t) - \mathrm{dens}(S') \;=\; \eta_S(t) - \mathrm{dens}(S)\,.$$

(2) *If, in addition,* $\mathrm{dens}(S) = \mathrm{dens}(\varGamma)/2$, *then the sets S and $S' = \varGamma\setminus S$ are homometric.*

(3) *The diffraction spectra of the sets S and S' are related by*

$$\widehat{\gamma}_{S'} \;=\; \widehat{\gamma}_S + \big(\mathrm{dens}(S') - \mathrm{dens}(S)\big)\,\mathrm{dens}(\varGamma)\,\delta_{\varGamma^*}\,.$$

In particular, $\widehat{\gamma}_{S'} = \widehat{\gamma}_S$ if $\mathrm{dens}(S') = \mathrm{dens}(S)$.

(4) *The diffraction measure $\widehat{\gamma}_{S'}$ is pure point if and only if $\widehat{\gamma}_S$ is pure point.*

Proof. In what follows, each term involving a density is to be viewed as the limit along a fixed increasing and unbounded sequence of radii, as in (24). Since $\varGamma$ is the disjoint union of S and S', $\varGamma = S \,\dot\cup\, S'$, we get $\mathrm{dens}(S') = \mathrm{dens}(\varGamma) - \mathrm{dens}(S)$ and the natural density of S' exists because $\mathrm{dens}(S) = \eta_S(0)$. Since $S' \subset \varGamma$, we also have $\eta_{S'}(z) = 0$ whenever $z \notin \varGamma$.

So, let $z = t \in \varGamma$ from now on. Next, observe that $\varGamma \cap (t + \varGamma) = \varGamma$ and thus, using $\varGamma = S \dot{\cup} S'$, we obtain

$$\begin{aligned} \operatorname{dens}(\varGamma) &= \operatorname{dens}\bigl(\varGamma \cap (t + \varGamma)\bigr) \\ &= \eta_{S'}(t) + \eta_S(t) + \operatorname{dens}\bigl(S \cap (t + S')\bigr) + \operatorname{dens}\bigl(S' \cap (t + S)\bigr). \end{aligned}$$

Since $S' = \varGamma \setminus S$, it is easy to verify that

$$\begin{aligned} \operatorname{dens}\bigl(S' \cap (t + S)\bigr) &= \operatorname{dens}\bigl(\varGamma \cap (t + S)\bigr) - \operatorname{dens}\bigl(S \cap (t + S)\bigr) \\ &= \operatorname{dens}(S) - \eta_S(t) \end{aligned}$$

because $(t + S) \subset \varGamma$ and $\operatorname{dens}(t + S) = \operatorname{dens}(S)$. Similarly,

$$\operatorname{dens}\bigl(S \cap (t + S')\bigr) \; = \; \operatorname{dens}(S) - \eta_S(-t)\,,$$

by first shifting (by $-t$) and then using the previous formula. Since $\eta_S(t)$ is a positive definite real function, we have $\eta_S(-t) = \eta_S(t)$, and obtain

$$\operatorname{dens}(\varGamma) \; = \; 2\operatorname{dens}(S) + \eta_{S'}(t) - \eta_S(t)$$

from which the first assertion follows with $\operatorname{dens}(\varGamma) = \operatorname{dens}(S) + \operatorname{dens}(S')$.

If $\operatorname{dens}(S) = \operatorname{dens}(\varGamma)/2$, then $\operatorname{dens}(S') = \operatorname{dens}(S)$ and we obtain $\eta_{S'}(z) = \eta_S(z)$, for all z, by the first assertion. This settles assertion (2).

Since $S \subset \varGamma$, its autocorrelation is $\gamma_S = \sum_{t \in \varGamma} \eta_S(t)\delta_t$, and analogously for S', the complement set in $\varGamma$. From the first assertion, we then infer

$$\gamma_{S'} \; = \; \gamma_S + c\,\delta_{\varGamma}$$

with $c = \operatorname{dens}(S') - \operatorname{dens}(S)$. Assertion (3) now follows from taking the Fourier transform and applying Poisson's summation formula to the lattice Dirac comb $\delta_{\varGamma}$.

Finally, the difference between $\widehat{\gamma}_{S'}$ and $\widehat{\gamma}_S$ in the third assertion is a multiple of $\delta_{\varGamma^*}$ which is a uniform lattice Dirac comb and hence a pure point measure, whence the last claim is obvious. □

In [13], it was shown that the set of visible lattice points is pure point diffractive. The last assertion of Theorem 4 then tells us that their complement, the set of *invisible* points, is pure point diffractive, too. Similarly, the set of k-th power free integers, a subset of $\mathbb{Z}$, has pure point diffraction [13], so does then its complement, the set of integers divisible by the k-th power of some integer ≥ 2. This indicates that many more pure point diffractive point sets of independent interest exist, and a general criterion based on the almost periodicity of the autocorrelation measure is derived in [12], see [30] for general background material.

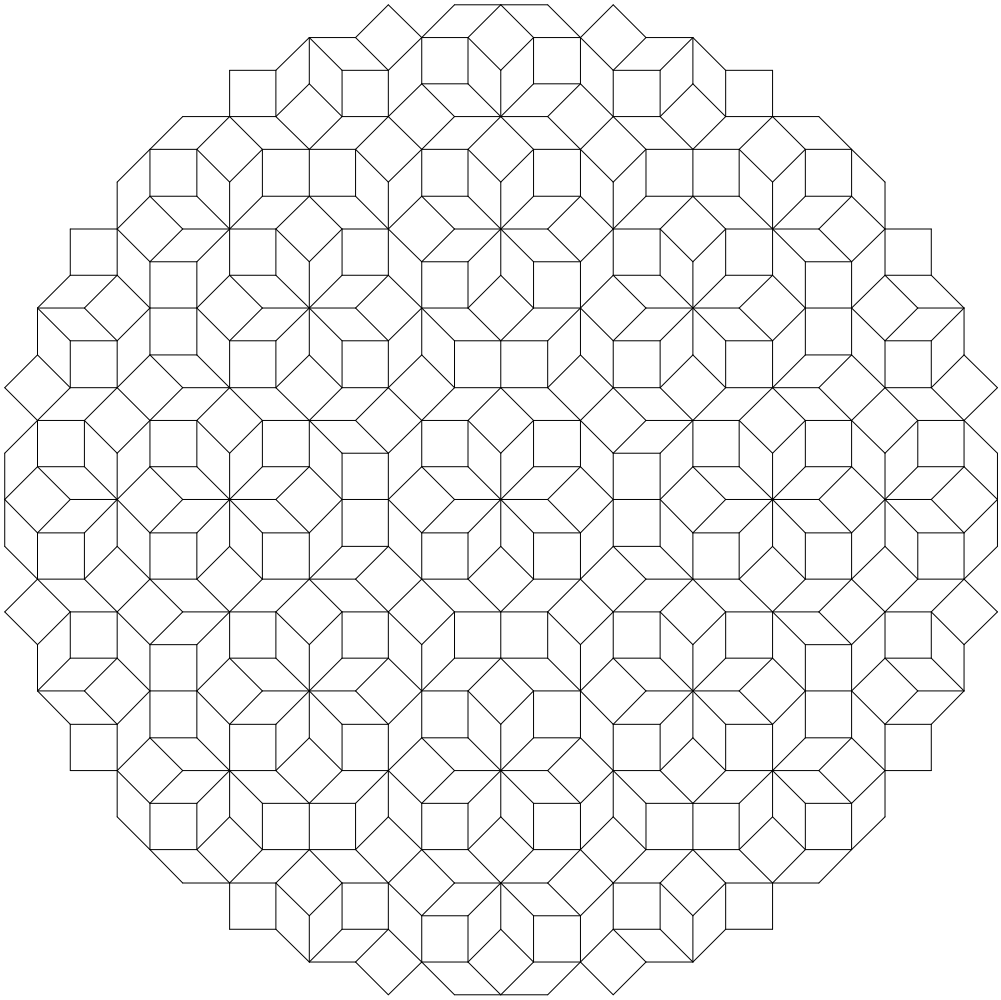

FIGURE 1. Central patch of the exactly eightfold symmetric Ammann–Beenker tiling. Its set of vertices is a model set, on the basis of the primitive cubic lattice $\mathbb{Z}^4$, with a regular octagon as the window.

3. Model sets

Model sets probably form the most important class of examples of aperiodic order. In their case, one starts with a periodic structure in a high-dimensional space and considers a partial "image" in a lower dimensional space. In general, this image will not be periodic any more but still preserves many regularity features due to the periodicity of the underlying high dimensional structure. For a survey and further references, we refer the reader to [52]; a gentle introduction, with many illustrations, is given in [6]. This reference is reprinted separately after this article, wherefore the following exposition on model sets is kept rather short to avoid duplications.

3.1. **Cut and project schemes.** Let us start with a brief recapitulation of the setting of a cut and project scheme and the definition of a model set. We need two locally compact Abelian groups, G and H, where G is also assumed to be σ-compact, see [64] for the reasons why this is needed. If $G = \mathbb{R}^n$, which is the case we are have in mind here, this condition is satisfied. Often, also H is a Euclidean space, but, already for the physically relevant theory, one needs an extension. As usual, neutral elements will be denoted by 0 (or by $0_G, 0_H$, if necessary). A *cut and project scheme* emerges out of the following collection of groups and mappings:

$$\begin{array}{ccccc} G & \xleftarrow{\pi} & G \times H & \xrightarrow{\pi_{\mathrm{int}}} & H \\ \cup & & \cup & & \cup\,\text{dense} \\ L & \xleftarrow{1-1} & \mathbb{L} & \longrightarrow & L^\star \\ \| & & & & \| \\ L & & \xrightarrow{\quad\star\quad} & & L^\star \end{array} \tag{25}$$

Here, $\mathbb{L}$ is a *lattice* in $G \times H$, i.e., a cocompact discrete subgroup. The canonical projection π is one-to-one between $\mathbb{L}$ and L (in other words, $\mathbb{L} \cap \big(\{0_G\} \times H\big) = \{0\}$), and the image $L^\star = \pi_{\mathrm{int}}(\mathbb{L})$ is dense in H. The group H is usually called the internal space. In view of the properties of the projections π and π_{int}, one usually defines the $\star$-map as $(.)^\star \colon L \longrightarrow H$ via $x^\star := \big(\pi_{\mathrm{int}} \circ (\pi|_{\mathbb{L}})^{-1}\big)(x)$, where $(\pi|_{\mathbb{L}})^{-1}(x) = \pi^{-1}(x) \cap \mathbb{L}$, for all $x \in L$.

A *model set* is now any translate of a set of the form

$$\curlywedge(W) \;:=\; \{x \in L \mid x^\star \in W\} \tag{26}$$

where the *window* W is a relatively compact subset of H with non-empty interior. Without loss of generality, we may assume that the stabilizer of the window,

$$H_W \;:=\; \{c \in H \mid c + W = W\}\,, \tag{27}$$

is the trivial subgroup of H, i.e., $H_W = \{0_H\}$. If this were not the case (which could happen in compact groups H for instance), one could factor by H_W and reduce the cut and project scheme accordingly [64, 10]. Furthermore, we may assume that $\langle W - W\rangle$, the subgroup of H that is algebraically generated by the subset $W - W$, is the entire group, i.e., $\langle W - W\rangle = H$, again by reducing the cut and project scheme to this situation if necessary, see [63] for details. An example is shown in Figure 1. This is the eightfold symmetric relative of the Penrose tiling, known as the Ammann-Beenker tiling.

3.2. **Diffraction from model sets.** There are variations on the precise requirement to W which depend on the fine properties of the model sets one is interested in, compare [52, 64]. In particular, a model set is called *regular* if ∂W has Haar measure 0 in H, and *generic* if, in addition, $\partial W \cap L^\star = \varnothing$. It is one of the central results of this area, compare [52, 64] and references given there, that (regular) model sets provide a very natural generalization of the concept of a lattice.

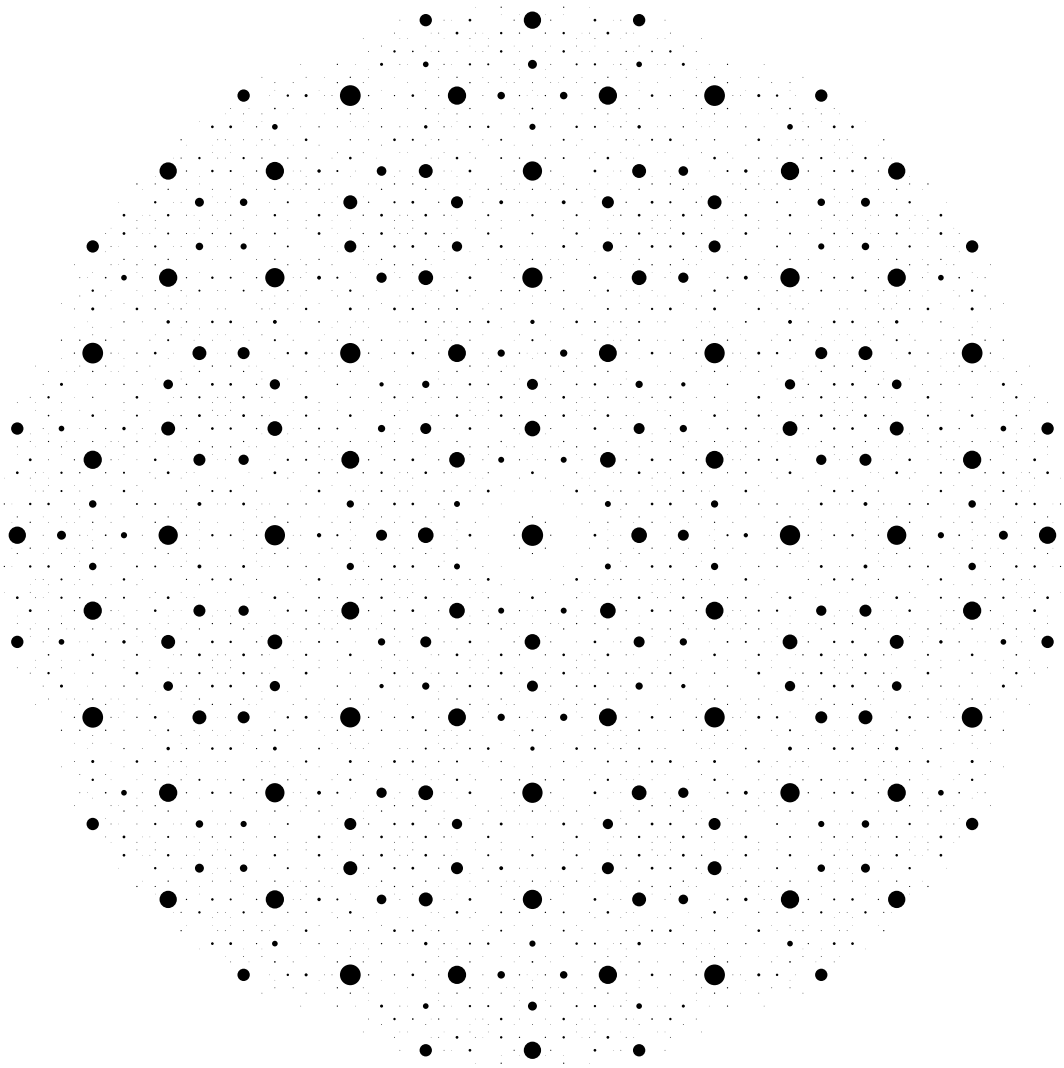

FIGURE 2. Diffraction image of the Ammann–Beenker tiling of Figure 1, with points of equal scattering strength on its vertices. A Bragg peak is displayed by a small disk, such that its centre is the location and its area the intensity of the peak. The locations of all Bragg peaks form a dense set of the plane, of which only finitely many (per unit area) are shown here (peaks with an intensity below 0.001 of the central intensity are suppressed).

Theorem 5. [64, 12] *Regular model sets are pure point diffractive.* □

This result was implicitly formulated soon after the discovery of quasicrystals. In fact, it is relatively easy to come up with an explicit formula for the pure point part of the diffraction measure in the standard Euclidean setting. However, it is then still a formidable task to prove the absence of other spectral components, and this was only achieved much later, see [36, 64] for the standard approach via dynamical systems and [12] for an independent proof on the basis of almost periodicity. The dynamical systems approach has recently also led to a better understanding of the connection between dynamical and diffraction spectra, see [8] and references given there for a survey.

Rather than displaying the proof here, let us summarize how to actually calculate the diffraction measure of a regular model set, for the case that $G = \mathbb{R}^n$ and $H = \mathbb{R}^m$. Then, $\mathbb{L}$ is a lattice of dimension $n+m$, with dual lattice $\mathbb{L}^*$. If we consider the Dirac comb $\delta_\varLambda$ for a regular model set $\varLambda = \curlywedge(W)$, its diffraction measure is unique and given by

$$\widehat{\gamma}_\varLambda \;=\; \sum_{k\in\mathbb{L}^*} |a(k)|^2\, \delta_{\pi_{\mathrm{int}}(k)} \tag{28}$$

with the Fourier-Bohr coefficient (or amplitude)

$$a(k) \;=\; \frac{\mathrm{dens}(\varLambda)}{\mathrm{vol}(W)} \int_W e^{2\pi i(\pi_{\mathrm{int}}(k)\cdot y)}\, \mathrm{d}y\,. \tag{29}$$

The normalization is chosen such that $a(0) = \mathrm{dens}(\varLambda)$, in line with standard conventions. Consequently, the central Bragg peak in (28) has intensity $|\mathrm{dens}(\varLambda)|^2$. Formula (29) has a natural extension to more general internal spaces as well, but we skip further details here. As in illustration, the diffraction of the Ammann-Beenker tiling of Figure 1 is shown in Figure 2.

For our purposes, it is sufficient to restrict our attention to regular model sets where W is a compact subset of H with $\overline{W^\circ} = W$ (in particular, W then has non-empty interior and, due to regularity, a boundary of Haar measure 0). This is motivated by the fact that diffraction cannot distinguish two model sets $\curlywedge(W)$ and $\curlywedge(W')$ if the symmetric difference $W \triangle W'$ of the windows has Haar measure 0 in H.

3.3. **Deformed model sets.** There is a class of important variants of the model sets just described that is obtained by a certain deformation. The latter modifies the structure considerably, but does not destroy the pure point diffractivity. In particular, the positions of the Bragg peaks remain unchanged, though their intensities are modified. Such sets are called *deformed model sets*, and were first investigated by Hof [36, 37], and later generalized considerably [19, 9].

A regular model set $\varLambda$ with compact window W can be deformed as follows [36, 19]. Let $\vartheta\colon W \longrightarrow G$ be a continuous mapping. If $\varLambda = \curlywedge(W)$, one defines

$$\varLambda_\vartheta \;:=\; \{x + \vartheta(x^\star) \mid x \in \varLambda\} \;=\; \{x + \vartheta(x^\star) \mid x \in L \text{ and } x^\star \in W\}\,, \tag{30}$$

usually subject to the extra requirement (on ϑ) that the point set $\varLambda_\vartheta$ defined this way is still uniformly discrete. One can avoid this condition by a measure-valued formulation, compare [9] for details.

Note that $\varLambda_\vartheta$, under the conditions mentioned, has a well defined density, $\mathrm{dens}(\varLambda_\vartheta) = \mathrm{dens}(\varLambda)$, which is thus unchanged by the deformation. Moreover, this approach permits a link to the theory of dynamical systems again, and to the theory of factors in particular, which is strong enough to prove the following result, see [54] for general background material and [9] for details of this approach to deformed model sets.

Theorem 6. [9] *Let $\varLambda$ be a regular model set for the cut and project scheme* (25)*, and let $\vartheta\colon H \longrightarrow G$ be a continuous mapping with compact support. Let $\varLambda_\vartheta$ be defined according to* (30)*, with the restriction that it is still uniformly discrete. Then, the diffraction measure of $\delta_{\varLambda_\vartheta}$ is a pure point measure.* □

As in the case of $\varLambda$, Bragg peaks can only exist on points of $\pi_{\mathrm{int}}(\mathbb{L}^*)$, where $\mathbb{L}^*$ is the dual lattice of $\mathbb{L}$ from the cut and project scheme (25). In fact, in the Euclidean case, the diffraction formula (28) remains valid, if one replaces the Fourier-Bohr coefficients $a(k)$ by their 'deformed' variants, $a_\vartheta(k)$, where

$$a_\vartheta(k) \;=\; \frac{\mathrm{dens}(\varLambda)}{\mathrm{vol}(W)} \int_W e^{2\pi i(\pi_{\mathrm{int}}(k)\cdot y - \pi(k)\cdot\vartheta(y))}\,\mathrm{d}y\,. \tag{31}$$

Note that $a_\vartheta(0) = \mathrm{dens}(\varLambda)$, in line with our previous remark on the density of the deformed model set.

4. Lattice systems with disorder

In what follows, we analyze the diffraction measure of translation invariant Ising type models on $\mathbb{Z}^d$, interpreted as lattice gases. More specifically, we consider models with single spin space $\{-1, 1\}$ and pair potentials which can be described by a real symmetric function $J(x) = J(-x)$ for $x \in \mathbb{Z}^d$ (so the corresponding Hamiltonian can formally be written as $H = -\sum_{x,y\in\mathbb{Z}^d} J(x-y)\sigma_x\sigma_y$, where $\sigma_x \in \{-1, +1\}$ denotes the spin at $x \in \mathbb{Z}^d$).

4.1. **General setting.** For a finite subsystem, $\mathbb{T} \subset \mathbb{Z}^d$ (with periodic boundary conditions, say), the partition function in the spin-formulation is

$$Z_\beta \;=\; \sum_{\{\boldsymbol{\sigma}\}} \exp(\,\beta \cdot \sum_{x,y\in\mathbb{T}} J(x-y)\,\sigma_x\,\sigma_y\,),$$

where $\beta = 1/(k_B T)$ is the inverse temperature, with Boltzmann's constant k_B, and the sum runs over all configurations $\boldsymbol{\sigma} = \{\sigma_x \,|\, x \in \mathbb{T}\}$ on $\mathbb{T}$. Via

$$\mu_\beta(\boldsymbol{\sigma}) \;=\; \frac{1}{Z_\beta}\,\exp(\,\beta \cdot \sum_{x,y\in\mathbb{T}} J(x-y)\,\sigma_x\,\sigma_y\,), \tag{32}$$

one defines a probability measure on the (finite) configuration space. In the infinite volume (or thermodynamic) limit, this leads to the corresponding *Gibbs measure*, compare [66] for details. The set of Gibbs measures is a non-empty simplex (see [29, Thm. 7.26]), but it need not be a singleton set. If its nature changes as a function of β (e.g., from a singleton to a 1-simplex), the system undergoes a second order phase transition. The point where this happens is $\beta_c = 1/(k_B T_c)$, the so-called *inverse critical temperature*. In the following, we shall only consider cases where the Gibbs measure is unique, i.e., where we have a singleton set. Since extremal Gibbs measures are ergodic (see [29, Thm. 14.15]), the unique Gibbs measure is ergodic, and quantities obtained as an average over the ensemble (such as the correlation functions which we consider next) are valid almost surely for each member of the ensemble, i.e., for each realization of the underlying stochastic process (with respect to the Gibbs measure). For a suitable exposition of the underlying ergodic theorem used here, we refer to [44].

Assuming uniqueness of the (translation invariant) Gibbs measure, the *density-density correlation function* $\langle n_0\, n_x\rangle_\beta$ in the lattice gas interpretation of the models considered can be deduced from $n_x = \frac{1}{2}(\sigma_x + 1)$, where the site x is occupied by a particle iff $n_x = 1$. This leads to the following relationship among the correlation functions (note that we assume uniqueness of the Gibbs measure, which implies $\langle \sigma_x\rangle_\beta = 0$):

$$\langle n_0\, n_x\rangle_\beta \;=\; \frac{1}{4} + \frac{\langle \sigma_0\, \sigma_x\rangle_\beta}{4}. \tag{33}$$

This interpretation yields the following positive definite autocorrelation *measure* (almost surely, in the sense explained above)

$$\gamma \;=\; \sum_{x\in\mathbb{Z}^d} \langle n_0\, n_x\rangle_\beta \, \delta_x \,.$$

As before, we are interested in the positive measure $\widehat{\gamma}$ and its decomposition as

$$\widehat{\gamma} \;=\; (\widehat{\gamma})_{\mathrm{pp}} + (\widehat{\gamma})_{\mathrm{sc}} + (\widehat{\gamma})_{\mathrm{ac}}$$

with respect to Lebesgue measure, i.e., our reference measure for volume elements of $\mathbb{R}^d$.

The constant part of (33) results in the pure point measure

$$(\widehat{\gamma})_{\mathrm{pp}} \;=\; \frac{1}{4}\cdot \sum_{k\in\mathbb{Z}^d} \delta_k \;=\; \frac{1}{4}\, \delta_{\mathbb{Z}^d} \tag{34}$$

in the diffraction measure (note that $\mathbb{Z}^d$ is self-dual), as a consequence of the PSF for distributions, see Proposition 2. Strictly speaking, the validity of (34) is not clear at this stage, we have only shown that $(\widehat{\gamma})_{\mathrm{pp}}$ "contains" $\frac{1}{4}\,\delta_{\mathbb{Z}^d}$. However, it is valid if $\frac{1}{4}\sum_{x\in\mathbb{Z}^d}\langle \sigma_0\,\sigma_x\rangle_\beta\,\delta_x$ is a null weakly almost periodic measure, see [30, Chapter 11]. This is true of the present example, and also of our later ones.

We shall now show that, in addition to this pure point part, almost surely only an absolutely continuous part is present in the diffraction measure of models on $\mathbb{Z}^d$ with finite-range "ferromagnetic" (i.e., attractive) two-body interactions for all temperatures above T_c. We shall also show that the same holds for models (deep) in the Dobrushin uniqueness regime that satisfy an additional condition on the rate of decay of their potential. Similar observations have also been made in [69, 7]. In view of the widespread application of such lattice gas models to disordered phenomena in solids, this gives a partial justification why singular continuous spectra are usually not considered in classical crystallography.

4.2. **Fourier series of decaying correlations.** Let us assume that the correlation coefficients of a model considered is either exponentially or algebraically decaying. We first look at exponentially decaying correlations, i.e.,

$$|\langle \sigma_0 \, \sigma_x \rangle_\beta| \;\leq\; C \cdot \mathrm{e}^{-\varepsilon \, \|x\|}, \tag{35}$$

where C, ε are positive constants depending only on β and the model considered, and $\|\cdot\|$ denotes the Euclidean norm, i.e., $\|x\|^2 = x_1^2 + \ldots + x_d^2$.

We shall now deduce from the absolute convergence of $\sum_{x\in\mathbb{Z}^d} \mathrm{e}^{-\varepsilon\,\|x\|}$ that the exponentially decaying part of the correlation yields an absolutely continuous part in the diffraction measure. From the inequality

$$|x_1| + \ldots + |x_d| \;\leq\; \sqrt{d} \cdot \|x\|,$$

we get

$$\begin{aligned}\sum_{x\in\mathbb{Z}^d} \mathrm{e}^{-\varepsilon\,\|x\|} &\leq \sum_{x\in\mathbb{Z}^d} \mathrm{e}^{-\frac{\varepsilon}{\sqrt{d}}\,(|x_1|+\ldots+|x_d|)} = \left(\sum_{n\in\mathbb{Z}} \mathrm{e}^{-\frac{\varepsilon}{\sqrt{d}}\,|n|}\right)^d \\ &= \left(\frac{\mathrm{e}^{\varepsilon/\sqrt{d}}+1}{\mathrm{e}^{\varepsilon/\sqrt{d}}-1}\right)^d = \left(\coth\left(\frac{\varepsilon}{2\sqrt{d}}\right)\right)^d .\end{aligned}$$

So far, we thus have

Lemma 3. *If the correlation coefficients is bounded as in* (35)*, the sum* $\sum_{x\in\mathbb{Z}^d}\langle\sigma_0\,\sigma_x\rangle_\beta$ *is absolutely convergent.* □

A similar result can also be proved for correlations with suitable algebraic (power law) decay, see [15] for details. The natural next step is

Proposition 6. *The diffraction measure of a lattice gas model on* $\mathbb{Z}^d$*, with correlation coefficients bounded as in* (35)*, almost surely exists, is* $\mathbb{Z}^d$*-periodic and consists of the pure point part of* (34) *and an absolutely continuous part with smooth density. No singular continuous part is present.*

Proof. Lattice gas models can also be treated as weighted lattice Dirac combs (with weight 1 if a site is occupied by a particle and weight 0 otherwise). So, the diffraction measure $\widehat{\gamma}$ can be represented as

$$\widehat{\gamma} = \varrho * \delta_{\mathbb{Z}^d}$$

with a finite positive measure ϱ that is supported on a fundamental domain of $\mathbb{Z}^d$, by an application of Theorem 3. This yields the $\mathbb{Z}^d$-periodicity, which is also implied by the following more explicit arguments.

We have already treated the pure point part in (34), which is adequate here due to the assumptions made on the correlation coefficients: Lemma 3 implies that the positive measure $\sum_{x\in\mathbb{Z}^d} \left|\langle\sigma_0\sigma_x\rangle_\beta\right| \delta_x$ is a finite measure, so has vanishing volume mean.

Since the sum $\sum_{x\in\mathbb{Z}^d}\langle\sigma_0\,\sigma_x\rangle_\beta$ is absolutely convergent, we can view the correlation coefficients $\langle\sigma_0\,\sigma_x\rangle_\beta$ as functions in $L^1(\mathbb{Z}^d)$. Their Fourier transforms are uniformly converging Fourier series (by the Weierstraß M-test) and are therefore continuous functions on $\mathbb{R}^d/\mathbb{Z}^d$, see [59, Theorem 1.2.4(a)], which are then also in $L^1(\mathbb{R}^d/\mathbb{Z}^d)$. Applying the Radon-Nikodym theorem finishes the proof. In fact, exponential decay implies that the Radon-Nikodym density is C^∞. □

4.3. **Lattice gases with short-range interactions.** The crucial step is now to find a large and relevant class of models with exponentially decaying correlations. One is provided by lattice gases with finite-range ferromagnetic two-body interaction, where the assumptions of Lemma 3 are satisfied, so that the diffraction can be analyzed by means of Proposition 6. Another is given by the large class of systems in the so-called Dobrushin uniqueness regime, see [15] and literature given there for further details. We summarize the situation for the former class as follows.

Theorem 7. [15] *For $\beta < \beta_c$ ($T > T_c$), the diffraction measure of a lattice gas model on $\mathbb{Z}^d$ with finite-range ferromagnetic two-body interaction almost surely exists, is $\mathbb{Z}^d$-periodic and consists of the pure point part $(\widehat{\gamma})_{\mathrm{pp}} = \frac{1}{4}\,\delta_{\mathbb{Z}^d}$ and an absolutely continuous part whose Radon-Nikodym density is C^∞. No singular continuous part is present.* □

A similar result, i.e., $\widehat{\gamma} = (\widehat{\gamma})_{\mathrm{pp}} + (\widehat{\gamma})_{\mathrm{ac}}$ and thus absence of any singular continuous diffraction part, holds for all systems in the Dobrushin uniqueness regime, as the correlation functions then also fall rapidly enough with distance. This includes all systems with finite local state space and short range interaction for sufficiently high temperatures [29, 16], and many more. This is a clear indication that singular continuous spectra are rather untypical for lattice systems with short-range stochastic interaction.

One further qualitative property of the absolutely continuous component can be extracted without making additional assumptions. In our setting, we know inequality (35) and also that

$$\eta(x) \;=\; \langle\sigma_0\,\sigma_x\rangle_\beta \;=\; \langle\sigma_0\,\sigma_{-x}\rangle_\beta \;=\; \eta(-x)\,,$$

which follows from the positive definiteness of the autocorrelation. Consequently, one has

$$\left(\sum_{x\in\mathbb{Z}^d} \eta(x)\, \delta_x \right)\widehat{\ } \, (k) \;=\; \sum_{x\in\mathbb{Z}^d} \eta(x)\, \cos(2\pi k x)\,,$$

where the right hand side is a uniformly converging Fourier series of a $\mathbb{Z}^d$-periodic continuous function, as a consequence of Lemma 3. In fact, in our setting of exponential decay of $\eta(x)$, this function is C^∞. Since $\eta(x) \geq 0$ for all $x \in \mathbb{Z}^d$, this function has absolute maxima at $k \in \mathbb{Z}^d$ (viewed as the dual lattice of $\mathbb{Z}^d$).

Proposition 7. *Under the assumptions of Theorem* 7*, the absolutely continuous component of the diffraction measure is represented by a smooth function that assumes its maximal value at positions $k \in \mathbb{Z}^d$.* □

This result reflects the well-known qualitative property that the diffuse background (i.e., the continuous components) concentrates around the Bragg peaks if the effective (stochastic) interaction is attractive. Otherwise, the two components "repel" each other, as in the dimer models, see [21, 70] for details.

Remark: All results also hold – mutatis mutandis – for an arbitrary lattice $\varGamma \subset \mathbb{R}^d$, since there exists a bijective linear map $\varGamma \to \mathbb{Z}^d$, $x \mapsto Ax$ where $A \in \mathrm{GL}_d(\mathbb{R})$ (i.e., A is an invertible $d \times d$-matrix with coefficients in $\mathbb{R}$). E.g., we can interpret a finite-range model on $\varGamma$ with range R as finite-range model on $\mathbb{Z}^d$ with range (bounded by) $\|A\|_2 \cdot R$, where $\|\cdot\|_2$ denotes the spectral norm of the matrix A. The ferromagnetic two-body interaction $\tilde{J}(x) = \tilde{J}(-x) \geq 0$ on $\varGamma$ changes to $J(y) = \tilde{J}(A^{-1}y) = \tilde{J}(-A^{-1}y) = J(-y) \geq 0$ for $y \in \mathbb{Z}^d$.

4.4. **Example: Ising model as lattice gas.** Let us illustrate the above findings with one of the best analyzed models in statistical physics, the 2D Ising model without external field, in the lattice gas interpretation with scatterers of strength $s_{(i,j)} \in \{1, 0\}$. The partition function in the spin-formulation ($\sigma_{(i,j)} \in \{+1, -1\}$) reads as follows

$$Z_\beta \;=\; \sum_{\{\boldsymbol{\sigma}\}} \exp\left(\sum_{(i,j)} \sigma_{(i,j)} \left(K_1 \sigma_{(i+1,j)} + K_2 \sigma_{(i,j+1)} \right) \right)\,, \tag{36}$$

where we sum over all configurations $\{\boldsymbol{\sigma}\}$, to be understood as explained above, e.g., by first restricting it to a torus and then taking the thermodynamic limit to obtain a Gibbs measure. We consider the ferromagnetic case with coupling constants $K_\ell = \beta J_\ell > 0$, $\ell \in \{1, 2\}$, where β is inverse temperature, as before. The model undergoes a second order phase transition at $\kappa := \left(\sinh(2K_1)\sinh(2K_2)\right)^{-1} = 1$. It is common knowledge that, in the regime with coupling constants smaller than the critical ones (corresponding to $T > T_c$), the ergodic equilibrium state with vanishing magnetization m is unique, whereas above ($T < T_c$), there exist two extremal translation invariant equilibrium states, which are thus

ergodic [66, Ch. III.5]. In this case, we assume to be in the extremal state with positive magnetization $m = (1-\kappa^2)^{1/8}$.

The diffraction properties of the Ising model can be extracted from the known asymptotic behaviour [51, 71] of the autocorrelation coefficients. We first state the result for the isotropic case ($K_1 = K_2 = K$) and comment on the general case later.

Proposition 8. *Away from the critical point, the diffraction measure of the Ising lattice gas almost surely exists, is $\mathbb{Z}^2$-periodic and consists of a pure point and an absolutely continuous part with continuous density. The pure point part reads*

(1) $T > T_c$: $\quad (\widehat{\gamma}_\omega)_{\mathrm{pp}} = \frac{1}{4}\sum_{\boldsymbol{k}\in\mathbb{Z}^2} \delta_{\boldsymbol{k}}$

(2) $T < T_c$: $\quad (\widehat{\gamma}_\omega)_{\mathrm{pp}} = \rho^2 \sum_{\boldsymbol{k}\in\mathbb{Z}^2} \delta_{\boldsymbol{k}}$,

where the density ρ is the ensemble average of the number of scatterers per unit area. It is related to the magnetization m via $\rho = (m+1)/2$.

Proof. First, note that $s_{(i,j)} = (\sigma_{(i,j)}+1)/2$ and thus $\langle \sigma_{(i,j)} \rangle = m = 2\rho - 1$, so ρ varies between 1 and 1/2. The asymptotic correlation function of two spins at distance $R = \sqrt{x^2+y^2}$ (as $R \to \infty$) is [51]

$$\langle \sigma_{(0,0)} \sigma_{(x,y)} \rangle \;\simeq\; \begin{cases} c_1 \frac{e^{-R/c_2}}{\sqrt{R}}, & T > T_c \\ m^2 + c_3 \frac{e^{-2R/c_2}}{R^2}, & T < T_c, \end{cases} \tag{37}$$

with constants c_1, c_2 and c_3 depending only on K and T, see also [47, p. 51] and references given there for a summary. The pure point part $(\widehat{\gamma}_\omega)_{\mathrm{pp}}$ results directly from the Fourier transform of the constant part of γ_ω (by means of the PSF) as derived from the asymptotics of $\langle s_{(0,0)} s_{(x,y)} \rangle = (\langle \sigma_{(0,0)} \sigma_{(x,y)} \rangle + 2m + 1)/4$.

Observe, for the remaining contributions, that both sums, $\sum_{(x,y)\in\mathbb{Z}^2} e^{-R/c_2}/\sqrt{R}$ and $\sum_{(x,y)\in\mathbb{Z}^2} e^{-2R/c_2}/R^2$, converge absolutely, so we can view the corresponding correlation coefficients as functions in $L^1(\mathbb{Z}^2)$. Their Fourier transforms (which are uniformly converging Fourier series) are continuous functions on $\mathbb{R}^2/\mathbb{Z}^2$, see [59, §1.2.3], which are then also in $L^1(\mathbb{R}^2/\mathbb{Z}^2)$. Applying the Radon-Nikodym theorem finishes the proof. □

Remark: At the critical point, the correlation function $\langle \sigma_{(0,0)} \sigma_{(x,y)} \rangle$ is asymptotically proportional to $R^{-1/4}$ as $R \to \infty$ [71, 47]. Again, taking out first the constant part of γ_ω, we get the same pure point part as in Prop. 8 for $T > T_c$. However, for the remaining part of γ_ω, our previous convergence arguments fail. Nevertheless, using a theorem of Hardy [20, p. 97], we can show that the corresponding Fourier series still converges for $\boldsymbol{k} \notin \mathbb{Z}^2$ (a natural order of summation is given by shells of increasing radius). In particular, this remaining part of the autocorrelation measure is still null weakly almost periodic, so that its Fourier transform is a continuous measure, compare [30].

For $\boldsymbol{k} \in \mathbb{Z}^2$, where the Bragg peaks reside, the series diverges. But this can neither result in further contributions to the Bragg peaks (the constant part of γ_ω had already been taken

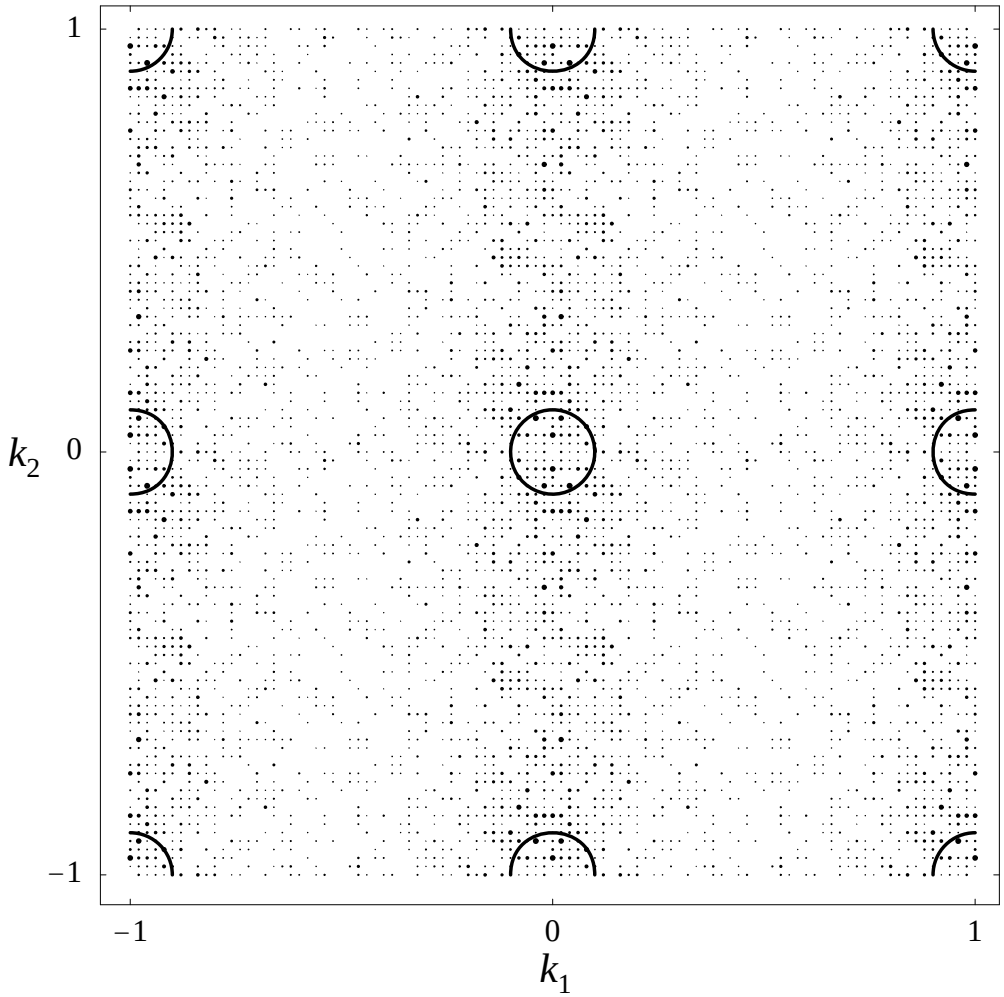

FIGURE 3. Diffraction image of a (slightly) non-isotropic Ising lattice gas on the square lattice. Bragg peaks are indicated by open circles, while the small black disks represent the absolutely continuous background, calculated numerically by means of fast Fourier transform from a periodic approximant.

care of) nor in singular continuous contributions (because the points of divergence form a uniformly discrete set). So, even though the series diverges for $\boldsymbol{k} \in \mathbb{Z}^2$, it still represents (we know that $\hat{\gamma}_\omega$ exists) a function in $L^1(\mathbb{R}^2/\mathbb{Z}^2)$ and hence the Radon-Nikodym density of an absolutely continuous background.

On the diffraction image, we can thus see, for any temperature, Bragg peaks on the square lattice and a $\mathbb{Z}^2$-periodic, absolutely continuous background concentrated around the peaks (the interaction is attractive). At the critical point, the intensity of the diffuse

scattering diverges when approaching the lattice positions of the Bragg peaks, but the qualitative picture remains the same.

The same arguments hold in the anisotropic case, where the asymptotics still conforms to Eq. (37) and the above, if $R = R(x, y)$ is replaced by the formula given in [71, Eq. 2.6]. The pure point part is again that of Prop. 8 with fourfold symmetry, while (as in the case of the domino tiling, see [7]) the continuous background breaks this symmetry if $K_1 \neq K_2$. This is illustrated in Figure 3, with $\boldsymbol{k} = (k_1, k_2)$ denoting the wave vector. Let us finally remark that a different choice of the scattering strengths (i.e. ± 1 rather than 1 and 0) would result in the extinction of the Bragg peaks in the disordered phase ($T > T_c$), but no choice does so in the ordered phase ($T < T_c$).

5. Random tilings

Another large and important class of models is formulated by means of *random tilings*. Here, starting from a finite number of proto-tiles (the "building blocks"), one considers all gapless and overlap-free coverings of larger and larger domains by copies of these proto-tiles. In the infinite volume limit, if the number of translationally inequivalent such coverings grow exponentially with the volume of the region, one speaks of a *random tiling ensemble*.

Such random tilings have many interesting features, see [32] for a comprehensive review. In particular, one has to carefully set up appropriate symmetry concepts and to link them together with entropic aspects of the ensemble [57]. Here, we want to consider some particularly simple cases from the diffraction point of view.

5.1. Binary random tilings in one dimension.

Our setting is that of a random tiling of the line with two intervals of length u and v, with prescribed frequencies p and q, respectively, where $p + q = 1$. We consider such a structure, and place a nomalized Dirac measure on all left endpoints of the intervals. The key parameter is then the length ratio $\alpha = u/v$. The diffraction of 1D random tilings has been investigated previously [7]. 1D binary random tilings have a non-trivial pure point part iff α is rational.

Theorem 8. [7] *Consider a random tiling of $\mathbb{R}$, built from two intervals of lengths u and v with corresponding probabilities p and q. Let $\varLambda$ denote the point set obtained from the left endpoints of the intervals of the tiling.*

The natural density of $\varLambda$ exists with probability 1 and is given by $d = (pu + qv)^{-1}$. If $\omega = \delta_{\varLambda} = \sum_{x \in \varLambda} \delta_x$ denotes the corresponding stochastic Dirac comb, the autocorrelation γ_ω of ω also exists with probabilistic certainty and is a positive definite pure point measure. The diffraction measure consists, with probabilistic certainty, of a pure point (Bragg) part and an absolutely continuous part, so $\widehat{\gamma}_\omega = (\widehat{\gamma}_\omega)_{\mathrm{pp}} + (\widehat{\gamma}_\omega)_{\mathrm{ac}}$.

If $\alpha = u/v$, the pure point part is

$$(\widehat{\gamma}_\omega)_{\mathrm{pp}} \;=\; d^2 \cdot \begin{cases} \delta_0\,, & \text{if } \alpha \notin \mathbb{Q}, \\ \sum_{k\in(1/\xi)\mathbb{Z}} \delta_k\,, & \text{if } \alpha \in \mathbb{Q}, \end{cases}$$

where, if $\alpha \in \mathbb{Q}$, we set $\alpha = a/b$ with coprime $a, b \in \mathbb{Z}$ and define $\xi = u/a = v/b$. The absolutely continuous part $(\widehat{\gamma}_\omega)_{\mathrm{ac}}$ can be represented by the continuous Radon-Nikodym density

$$g(k) \;=\; \frac{d \cdot pq\, \sin^2(\pi k\,(u-v))}{p\, \sin^2(\pi k\, u) + q\, \sin^2(\pi k\, v) - pq\, \sin^2(\pi k\,(u-v))},$$

which is well defined for $k\,(u-v) \notin \mathbb{Z}$. It has a smooth continuation to the excluded points. If α is irrational, this is $g(k) = 0$ for $k(u-v) \in \mathbb{Z}$ with $k \neq 0$ and

$$g(0) \;=\; \frac{d \cdot pq\,(u-v)^2}{p\,u^2 + q\,v^2 - pq\,(u-v)^2} \;=\; d\,\frac{pq\,(u-v)^2}{(p\,u+q\,v)^2}.$$

For $\alpha = a/b \in \mathbb{Q}$ as above, it is $g(k) = 0$ for $k\,(u-v) \in \mathbb{Z}$, but $k\,u \notin \mathbb{Z}$ (or, equivalently, $k\,v \notin \mathbb{Z}$), and

$$g(k) \;=\; d\,\frac{pq\,(a-b)^2}{(p\,a+q\,b)^2}$$

for the case that also $k\,u \in \mathbb{Z}$.

Proof. The statement about the density d is clear if one realizes that each random tiling can be viewed as a realization of a stochastic process of Bernoulli (or coin tossing) type, and the formula is then obvious. For the given realization, it is true with probability 1, see [27, 54] for background material.

For the diffraction, in view of the mixed spectral type, one has to determine the autocorrelation first. It is obvious that a gapless block of m tiles of type u and n of type v can be arranged in $\binom{m+n}{m}$ different ways. If u/v is irrational, $z = mu+nv$ does not permit any other decomposition into these tiles, so that the autocorrelation is given by

$$\gamma \;=\; d\Bigg(\delta_0 + \sum_{\substack{z>0 \\ z=mu+nv}} \binom{m+n}{m} p^m q^n \left(\delta_z + \delta_{-z}\right)\Bigg).$$

If u/v is rational, one can use the same formula, if the summation is then understood to also run over all possibilities to represent a given $z > 0$ as a sum of the form $mu+nv$, with $m, n \geq 0$. In both cases, this formula is obtained via the ensemble average. For a given realization, it is then valid with probability 1, because the underlying Bernoulli process is ergodic, compare [7, 54] for details.

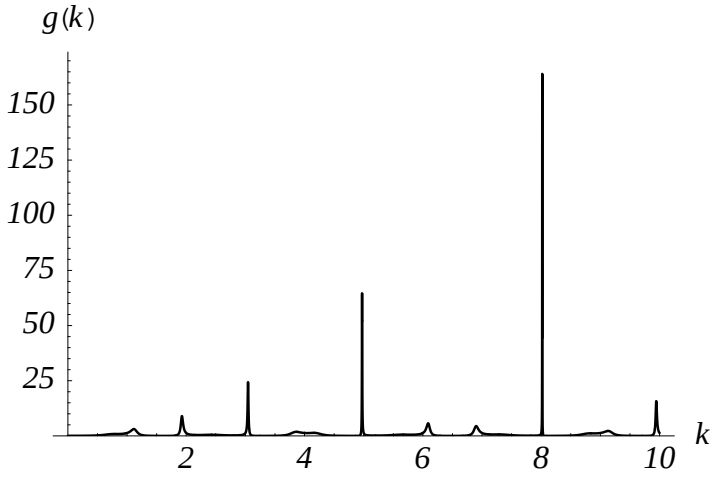

FIGURE 4. Absolutely continuous background of a typical Fibonacci random tiling.

The (formal) Fourier transform now reads

$$\widehat{\gamma} \;=\; d\biggl(1+2\sum_{\substack{z>0\\ z=mu+nv}}\binom{m+n}{m}p^m q^n\,\cos(2\pi i k z)\biggr)\,,$$

to be understood in the distribution sense. The analysis of this sum is not completely obvious, and requires a careful discussion of its points of convergence, divergence, and continuity, in dependence of u/v being irrational or not. This can be done by invoking geometric series arguments and results in the claims stated in the theorem, see [7] for the details. □

The most prominent 1D random tiling is the Fibonacci random tiling, where $u = \tau = (1+\sqrt{5})/2$ and $v = 1$, with occupation probabilities $p = 1/\tau$ and $q = 1-p = 1/\tau^2$ of the intervals (almost surely). Each interval endpoint of any realization of a Fibonacci random tiling belongs to the module $\mathbb{Z}[\tau] = \{m\tau + n \,|\, m, n \in \mathbb{Z}\}$. Every perfect Fibonacci tiling (as obtained from the cut and project method), also appears in the ensemble of the Fibonacci random tilings, but they are all "untypical" within this ensemble (i.e., their appearance has probability 0).

According to be above theorem, the diffraction measure comprises, with probabilistic certainty, a trivial Bragg peak at the origin and an absolutely continuous background, see Figure 4 for the latter. The absolutely continuous background, though being smooth, shows localized, bell-shaped needles of increasing height at sequences of points scaling with the golden ratio τ. This is reminiscent of the perfect Fibonacci tiling, where Bragg peaks line up in a similar fashion.

Clearly, this discussion can be extended to random tilings $\varLambda$ with more than two interval types as tiles. One obtains expressions with multinomial coefficients in return, and the appearance of Bragg peaks beyond the trivial one at $k = 0$ depends on the mutual commensurability of all interval lengths present. As soon as only one length ratio is irrational, only the trivial Bragg peak $\bigl(\mathrm{dens}(\varLambda)\bigr)^2\,\delta_0$ survives [7].

5.2. **Random tilings for $d \geq 2$.** Here, the picture is much less complete. For various planar systems from the theory of exactly solved models of statistical mechanics (see [68] for a very readable introduction to such models), one knows the autocorrelation sufficiently well [28, 71, 53], at least asymptotically, to determine the diffraction, again almost surely in the ensemble sense. This includes various dimer models [7, 33, 35].

One classic example is the planar random tiling built from rhombi with unit edge lengths and an opening angle of $\pi/3$, available in 3 different orientations. An example is shown in Figure 5. The corresponding ensemble is in one-to-one correspondence to the ensemble of fully packed dimer configurations with the hexagonal or honeycomb packing (i.e., the periodic repetition of a regular hexagon). This ensemble is known to have positive entropy density, compare [32, 57], with the maximal contribution from the realizations with 6-fold (and hence maximal) symmetry, the latter to be understood in the statistical (or ensemble) sense.

The dimer model on the honeycomb packing is an exactly solved and much studied model of statistical mechanics, see [28, 42, 43, 45, 46] and reference given there for further details. In particular, the ensemble is equipped with a unique Gibbs measure, parametrized by the frequencies of the tiles in the three orientations. This measure is thus an ergodic measure, and its correlations are rather well understood. With similar methods as used above for the diffraction of lattice gases, one can thus formulate and prove the following result [7], see also [15] for its embedding into a more general setting.

Theorem 9. *Consider a random lozenge tiling, with prescribed prototile frequencies ρ_i, $i \in \{1, 2, 3\}$, and let $\omega = \delta_{\varLambda}$ be the random Dirac comb obtained from the centres of the tiles. Then, the diffraction measure of ω exists with probability* 1*, and consists of a pure point and an absolutely continuous part. In particular, one has $\widehat{\gamma}_\omega = (\widehat{\gamma}_\omega)_{\mathrm{pp}} + (\widehat{\gamma}_\omega)_{\mathrm{ac}}$, with*

$$(\widehat{\gamma}_\omega)_{\mathrm{pp}} \;=\; \frac{4}{3} \sum_{\boldsymbol{k} \in \varGamma^*} \bigl((-1)^{k_1}\rho_1 + (-1)^{k_2}\rho_2 + \rho_3\bigr)^2\, \delta_{\boldsymbol{k}}, \tag{38}$$

where $\varGamma^*$ is the dual lattice of the triangular lattice, spanned by $\left(1, -\frac{1}{\sqrt{3}}\right)^t$ and $\left(0, \frac{2}{\sqrt{3}}\right)^t$. There is no singular continuous part, and $\widehat{\gamma}_\omega$ is fully periodic, with lattice of periods $2\varGamma^*$.

Proof. The autocorrelation γ is a positive and positive definite pure point measure, supported on the union of the triangular lattice $\varGamma$ and three of its cosets. For almost all realizations of the random tiling, by ergodicity of the underlying Gibbs measure, γ is of

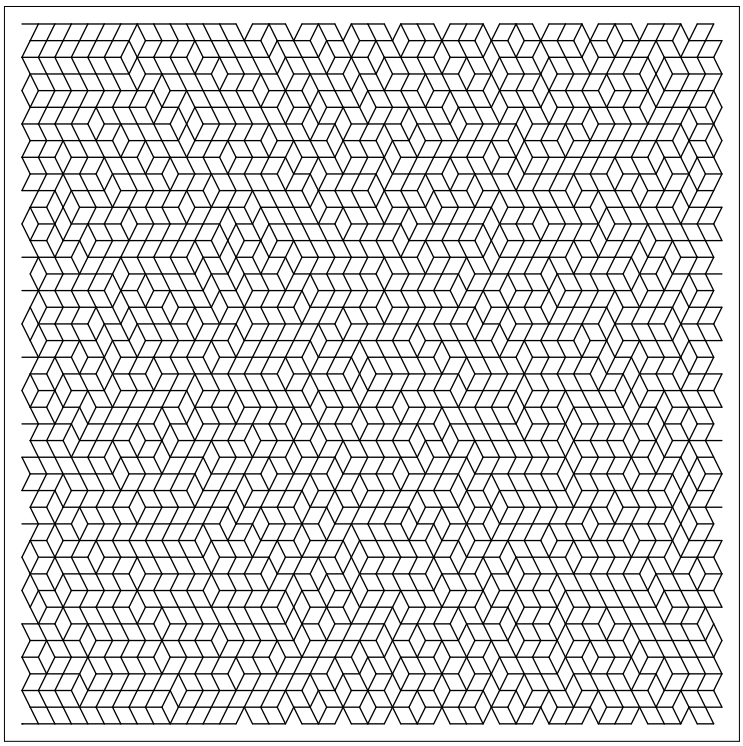

FIGURE 5. Typical patch of a rhombus (or lozenge) random tiling, with periodic boundary conditions. The frequencies of the three orientations differ (the vertical rhombi are less frequent than the other two types), so that this example does not have 6-fold (statistical) symmetry.

the form obtained by the usual ensemble average. Then, its coefficients can be split into a finite sum of constant parts (then being some combinations of density factors) and a covariance type part, the latter decaying algebraically with the distance from 0, see [72, 45, 7].

The pure point part of the diffraction measure, $\widehat{\gamma}_{\mathrm{pp}}$, is now simply the Fourier transform of the constant parts of γ emerging that way, again calculated by means of Poisson's summation formula for the triangular lattice $\varGamma$ and its modification for the involved translates of it (the latter simply giving an additional phase factor).

What remains, once again gives a Fourier series that converges to a function that is square integrable on a fundamental domain of $2\varGamma^*$, the latter also being its lattice of periods. By Hölder's inequality, this is then also an integrable function, and thus the Radon-Nikodym density of an absolutely continuous measure, see [7] for details. □

Figure 6 illustrates the diffraction image, which shows the symmetry correctly this time already on the level of the Bragg peaks alone. In the closely related square lattice dimer model, however, one would extract the correct symmetry only from the diffuse background, as in our earlier Ising lattice gas example. Further examples can be analyzed along similar

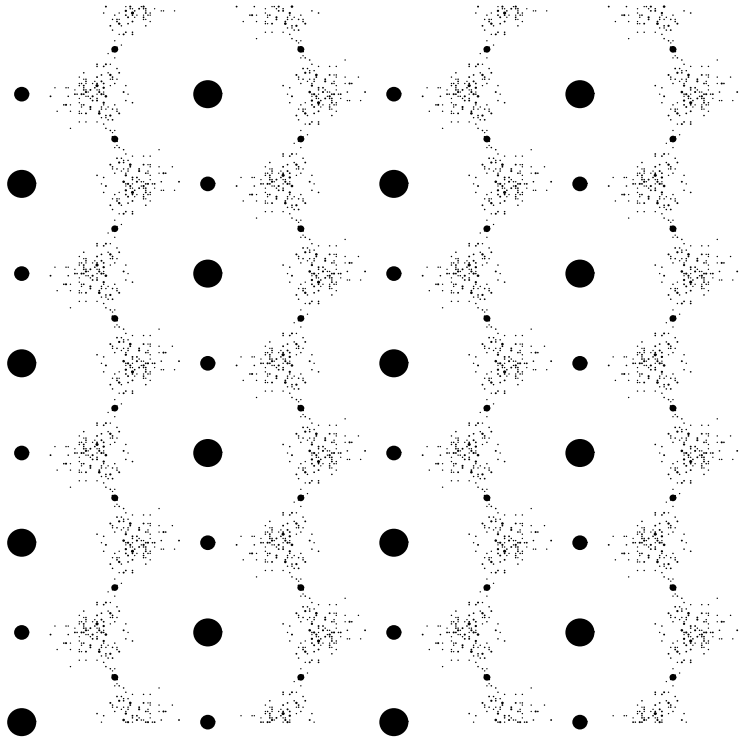

FIGURE 6. Diffraction image of the lozenge random tiling of Figure 5. The Bragg peaks are represented by the three types of large spots, while the smaller spots represent the absolutely continuous background, once again calculated numerically by fast Fourier transform of the periodic approximant.

lines, compare [33, 35] for a more complex case. As before, one can expand on the properties of the background, which turns out to have a continuous Radon-Nikodym density, see [15]. Also, its "repulsive" nature is clearly visible, and lines up with the repulsive nature of the effective interaction created by the stochastic process.

In a certain sense, this picture is rather satisfactory. Unfortunately, things change and get a lot more involved when one tries to get the analogous results for genuinely quasicrystalline random tiling ensembles, such as the randomized version of the Ammann-Beenker tiling of Figure 1. Here, it is still not completely clear what happens – and the planar case apparently is a critical one. As we have seen above, a generic one-dimensional random tiling produces an absolutely continuous diffraction image (apart from the trivial Bragg peak at $k = 0$). On the other hand, it is a long-standing conjecture that relevant random tilings in 3-space, such as the icosahedrally symmetric one built from the two classic Kepler rhombohedra, will produce a mixture of Bragg and absolutely continuous parts, see [32, 58] for details.

Based upon heuristic scaling arguments [32] and various numerical calculations [35], one expects the Ammann-Beenker random tiling with statistical 8-fold symmetry to show only the trivial Bragg peak at the origin, but otherwise a mixture of singular and absolutely continuous parts. From the geometric insight, due to a fluctuation argument in embedding space [32], it is also plausible that 2 really is the critical dimension for this phenomenon to happen, but it remains a challenge to prove (or disprove) this claim, in particular in view of the fact that scaling properties, in general, are not conclusive, see [39] for a discussion.

Acknowledgements. This survey is based on joint work with several people, including Moritz Höffe, Daniel Lenz, Robert V. Moody, Martin Schlottmann and Bernd Sing. It is my pleasure to thank them for their cooperation. Moreover, I want to thank Uwe Grimm and Natali Zint for helpful comments on the manuscript, and Gervais Chapuis for his hospitality and patience.

References

[1] L. Argabright and J. Gil de Lamadrid, *Fourier Analysis of Unbounded Measures on Locally Compact Abelian Groups*, Memoirs of the AMS, no. 145, AMS, Providence, RI (1974).

[2] J. Arsac, *Fourier Transforms and the Theory of Distributions*, Prentice Hall, Englewood Cliffs (1966).

[3] M. Baake, "A guide to mathematical quasicrystals", in: *Quasicrystals – An Introduction to Structure, Physical Properties, and Applications*, eds. J.-B. Suck, M. Schreiber and P. Häussler, Springer, Berlin (2001), pp. 17–48; `math-ph/9901014`.

[4] M. Baake, "Diffraction of weighted lattice subsets", *Can. Math. Bulletin* **45** (2002) 483–498; `math.MG/0106111`.

[5] M. Baake and D. Frettlöh, "SCD patterns have singular diffraction", *J. Math. Phys.* **46** (2005) 033510: 1–10; `math-ph/0411052`.

[6] M. Baake, U. Grimm and R. V. Moody, "What is aperiodic order?", `math.HO/0203252`.

[7] M. Baake and M. Höffe, "Diffraction of random tilings: Some rigorous results", *J. Stat. Phys.* **99** (2000), 219–261; `math-ph/9901008`.

[8] M. Baake and D. Lenz, "Dynamical systems on translation bounded measures: Pure point dynamical and diffraction spectra", *Ergodic Th. & Dynam. Syst.* **24** (2004) 1867–1893; `math.DS/0302231`.

[9] M. Baake and D. Lenz, "Deformation of Delone dynamical systems and topological conjugacy", *J. Fourier Anal. Appl.* **11** (2005) 125–150; `math.DS/0404155`.

[10] M. Baake, D. Lenz and R. V. Moody, "Characterization of model sets by dynamical systems", preprint (2005).

[11] M. Baake and R. V. Moody, "Diffractive point sets with entropy", *J. Phys. A: Math. Gen.* **31** (1998) 9023–9039; `math-ph/9809002`.

[12] M. Baake and R. V. Moody, "Weighted Dirac combs with pure point diffraction", *J. reine & angew. Math.* (*Crelle*) **573** (2004) 61–94; `math.MG/0203030`.
[13] M. Baake, R. V. Moody and P. A. B. Pleasants, "Diffraction from visible lattice points and kth power free integers", *Discr. Math.* **221** (2000) 3–42; `math.MG/9906132`.
[14] M. Baake, R. V. Moody and M. Schlottmann, "Limit-(quasi-)periodic point sets as quasicrystals with p-adic internal spaces" *J. Phys. A: Math. Gen.* **31** (1998) 5755–5765.
[15] M. Baake and B. Sing, "Diffraction spectrum of lattice gas models above T_c", *Lett. Math. Phys.* **68** (2004) 165–173; `math-ph/0405064`.
[16] M. Baake and N. Zint, "Absence of singular continuous diffraction spectra for multicomponent particle models of lattice gas type", in preparation.
[17] H. Bauer, *Maß- und Integrationstheorie*, 2nd ed., de Gruyter, Berlin (1992).
[18] S. K. Berberian, *Measure and Integration*, Macmillan, New York (1965).
[19] G. Bernuau and M. Duneau, "Fourier analysis of deformed model sets", in: *Directions in Mathematical Quasicrystals* eds. M. Baake and R. V. Moody, CRM Monograph Series, vol. 13, AMS, Providence, RI (2000), pp. 43–60.
[20] T. J. I'A. Bromwich, *An Introduction to the Theory of Infinite Series*, 2nd rev. ed., Macmillan, London (1965); reprint, Chelsea, New York (1991).
[21] J. M. Cowley, *Diffraction Physics*, 3rd ed., North-Holland, Amsterdam (1995).
[22] L. Danzer, "A family of 3D-spacefillers not permitting any periodic or quasiperiodic tiling", in: *Aperiodic '94*, eds. G. Chapuis and W. Paciorek, World Scientific, Singapore (1995), pp. 11–17.
[23] J. Dieudonné, *Treatise of Analysis*, vol. II, Academic Press, New York (1970).
[24] S. Dworkin, "Spectral theory and X-ray diffraction", *J. Math. Phys.* **34** (1993) 2965–2967.
[25] W. Ehm, T. Gneiting and D. Richards, "Convolution roots of radial positive definite functions with compact support", *Trans. AMS* **356** (2004) 4655–4685.
[26] V. Elser, "Comment on: Quasicrystals – A New Class of Ordered Structures", *Phys. Rev. Lett.* **54** (1985) 1730.
[27] W. Feller, *An Introduction to Probability Theory and its Applications*; vol. 1, 3rd ed., rev. printing, Wiley, New York (1970); vol. 2, 2nd ed., Wiley, New York (1991).
[28] M. E. Fisher and J. Stephenson, "Statistical mechanics of dimers on a plane lattice. II. Dimer correlations and monomers", *Phys. Rev.* **132** (1963) 1411–1431.
[29] H.-O. Georgii, *Gibbs Measures and Phase Transitions*, de Gruyter, Berlin (1988).
[30] J. Gil de Lamadrid and L. N. Argabright, *Almost Periodic Measures*, Memoires of the AMS, vol. **65**, no. 428, AMS, Providence, RI (1990).
[31] A. Guinier, *X-ray Diffraction in Crystals, Imperfect Crystals and Amorphous Bodies*, Freeman, San Francisco (1963); reprint: Dover, New York (1994).
[32] C. L. Henley, "Random tiling models", in: *Quasicrystals - The State of the Art*, eds. D. P. DiVincenzo and P. J. Steinhardt, 2nd ed., World Scientific, Singapore (1999), pp. 459–560.
[33] M. Höffe, "Diffraction of the dart-rhombus random tiling", *Mat. Science Eng. A* **294–296** (2000) 373–376; `math-ph/9911014`.
[34] M. Höffe and M. Baake, "Surprises in diffuse scattering", *Z. Kristallogr.* **215** (2000) 441–444; `math-ph/0004022`.

[35] M. Höffe, *Diffraktionstheorie stochastischer Parkettierungen*, Dissertation, Universität Tübingen, Shaker, Aachen (2001).
[36] A. Hof, "On diffraction by aperiodic structures", *Commun. Math. Phys.* **169** (1995) 25–43.
[37] A. Hof, "Diffraction by aperiodic structures", in: *The Mathematics of Long-Range Aperiodic Order*, ed. R. V. Moody, NATO ASI Series C 489, Kluwer, Dordrecht (1997), pp. 239–268.
[38] A. Hof, "Diffraction by aperiodic structures at high temperatures", *J. Phys. A: Math. Gen.* **28** (1995) 57–62.
[39] A. Hof, "On scaling in relation to singular spectra", *Commun. Math. Phys.* **184** (1997) 567–577.
[40] H. Jagodzinski and F. Frey, "Disorder diffuse scattering of X-rays and neutrons", in: *International Tables of Crystallography B*, ed. U. Shmueli, 2nd ed., Kluwer, Dordrecht (1996), pp. 392–433.
[41] M. V. Jarić and D. R. Nelson, "Diffuse scattering from quasicrystals", *Phys. Rev.* **B37** (1988) 4458–4472.
[42] P. W. Kasteleyn, "The statistics of dimers on a lattice", *Physica* **27** (1961) 1209–1225.
[43] P. W. Kasteleyn, "Dimer statistics and phase transitions", *J. Math. Phys.* **4** (1963) 287–293.
[44] G. Keller, *Equilibrium States in Ergodic Theory*, LMSST 42, Cambridge University Press, Cambridge (1998).
[45] R. Kenyon, "Local statistics of lattice dimers", *Ann. Inst. H. Poincaré Prob.* **33** (1997) 591–618.
[46] R. Kenyon, "The planar dimer model with boundary: a survey", in: *Directions in Mathematical Quasicrystals*, eds. M. Baake and R. V. Moody, CRM Monograph Series, vol. 13, AMS, Providence, RI (2000), pp. 307–328.
[47] R. Kindermann and J. L. Snell, *Markov Random Fields and their Applications*, Contemp. Mathematics, vol. 1, AMS, Providence, RI (1980).
[48] C. Külske, "Universal bounds for the selfaveraging of random diffraction measures", *Probab. Th. Rel. Fields* **126**(2002) 29–50; `math-ph/0109005`.
[49] J. C. Lagarias and P. A. B. Pleasants, "Repetitive Delone sets and quasicrystals", *Ergodic Th. & Dynam. Syst.* **23** (2003) 831–867; `math.DS/9909033`.
[50] S. Lang, *Real and Functional Analysis*, 3rd ed., Springer, New York (1993).
[51] B. M. McCoy and T. T. Wu, *The Two-Dimensional Ising Model*, Harvard University Press, Cambridge, MA (1973).
[52] R. V. Moody, "Model sets: A Survey", in: *From Quasicrystals to More Complex Systems*, eds. F. Axel, F. Dénoyer and J. P. Gazeau, EDP Sciences, Les Ulis, and Springer, Berlin (2000), pp. 145–166; `math.MG/0002020`.
[53] E. W. Montroll, "Lattice Statistics", in: *Applied Combinatorial Mathematics*, ed. E. F. Beckenbach, John Wiley, New York (1964), pp. 96–143.
[54] K. Petersen, *Ergodic Theory*, Cambridge University Press, Cambridge (1983).
[55] M. Queffélec, "Spectral study of automatic and substitutive sequences", in: *Beyond Quasicrystals*, eds. F. Axel and D. Gratias, Springer, Berlin (1995), pp. 369–414.
[56] M. Reed and B. Simon, *Methods of Modern Mathematical Physics I: Functional Analysis*, 2nd ed., Academic Press, San Diego (1980).

[57] C. Richard, M. Höffe, J. Hermisson and M. Baake, "Random tilings – concepts and examples", *J. Phys. A: Math. Gen.* **31** (1998) 6385–6408; `cond-mat/9712267`.
[58] C. Richard, "Dense Dirac combs in Euclidean space with pure point diffraction", *J. Math. Phys.* **44** (2003) 4436–4449; `math-ph/0302049`.
[59] W. Rudin, *Fourier Analysis on Groups*, Wiley Interscience, New York (1962).
[60] W. Rudin, *Functional Analysis*, 2nd ed., McGraw-Hill, New York (1991).
[61] D. Ruelle, *Statistical Mechanics: Rigorous Results*, Addison Wesley, Redwood City (1969).
[62] D. Ruelle, "Do turbulent crystals exist?", *Physica* **113 A** (1982) 619–623.
[63] M. Schlottmann, "Cut-and-project sets in locally compact Abelian groups", in: *Quasicrystals and Discrete Geometry*, ed. J. Patera, Fields Institute Monographs, vol. 10, AMS, Providence, RI (1998), pp. 247–264.
[64] M. Schlottmann, "Generalized model sets and dynamical systems", in: *Directions in Mathematical Quasicrystals*, eds. M. Baake and R. V. Moody, CRM Monograph Series, vol. 13, AMS, Providence, RI (2000), pp. 143–159;
[65] L. Schwartz, *Théorie des Distributions*, 3rd ed., Hermann, Paris (1998).
[66] B. Simon, *The Statistical Mechanics of Lattice Gases*, Vol. 1, Princeton University Press, Princeton (1993).
[67] N. Strungaru, "Almost periodic measures and long-range order in Meyer sets", *Discr. Comput. Geom.* **33** (2005) 483–505.
[68] C. J. Thompson, *Mathematical Statistical Mechanics*, Princeton University Press, Princeton (1972).
[69] A. C. D. van Enter and J. Miękisz, "How should one define a (weak) crystal?", *J. Stat. Phys.* **66** (1992) 1147–1153.
[70] T. R. Welberry, "Diffuse X-ray scattering and models of disorder", *Rep. Prog. Phys.* **48** (1985) 1543–1593.
[71] T. T. Wu, B. M. McCoy, C. A. Tracy and E. Barouch, "Spin-spin correlation functions for the two-dimensional Ising model: Exact theory in the scaling region", *Phys. Rev.* **B13** (1976) 316–374.
[72] R. Youngblood, J. D. Axe and B. M. McCoy, "Correlations in ice-rule ferroelectrics", *Phys. Rev.* **B21** (1980) 5212–5220.

Fakultät für Mathematik, Univ. Bielefeld, Postfach 100131, 33501 Bielefeld, Germany
E-mail address: `mbaake@math.uni-bielefeld.de`
URL: `http://www.math.uni-bielefeld.de/baake/`

What is Aperiodic Order?

Michael Baake, Uwe Grimm, Robert V. Moody

1 Introduction

Surely one of the most miraculous aspects of Nature is its self-organizing ability of creating solid substances with corresponding well-defined macroscopic properties (namely material objects of the world around us) using vast numbers of submicroscopic building blocks (namely atoms and molecules). Underlying this is the mystery of long-range order. Even putting aside the difficult kinematic questions about crystal growth, there remains a host of profound geometric problems: what do we mean by long-range order, how is it characterized, and how can we model it mathematically?

In crystals, like ice, sugar, and salt, many of the extraordinarily exact macroscopic features derive from a very simple geometric idea: the endless repetition of a (relatively) small pattern. A small arrangement of atoms forms a fundamental cell that constitutes a building block, copies of which are stacked together like bricks to fill out space by periodic repetition. Simple as this model is, it is still difficult to analyze in full mathematical detail: there are 230 possible symmetry classes (called space groups) theoretically available for such periodic cell arrangements, each of which is now also known to actually exist in Nature. However, it took almost 100 years from the theoretical classification of the 230 space groups to the experimental discovery of the last examples. Nonetheless, the underlying feature of all crystals, which appear ubiquitously in the natural world, is their pure periodic structure in three independent directions — their so-called lattice symmetry. The interesting thing is that there is striking long-range order in Nature that does not fit into this scheme, and one important example of this has only been discovered recently.

Early in the last century, the wonderful tool of X-ray diffraction was introduced, based on much older ideas of optical scattering (which is what we will use to explain its essence). Initially, diffraction pictures provided powerful evidence of the truth of the atomic theory of matter. Over the years, they have become a standard tool for analyzing crystals, and to detect long-rang order through the appearance of sharp reflection spots in the diffraction image. The basic idea can be visualized with an optical bench which is driven by a small laser as source for the coherent light (Box 1), see [3] for details on this, with many instructive examples.

Diffraction pictures of crystals display beautiful point-patterns that are symptomatic of the long-range repetitive lattice nature of the crystal. Sometimes these

pictures seem so crystal-like themselves that, at first sight, they might lead one to think that they rather directly mark the atomic positions. In fact, however, they display the symmetry of another lattice that is dual (or reciprocal) to the one underlying the crystal structure. (See Boxes 8 and 12 for more on this).

For almost 80 years, the point-like feature of the diffraction image seemed to be the characterizing property of crystals; so much so that the three concepts of lattice symmetry, crystal structure, and pure point diffraction were considered as synonymous. Thus it was a minor crisis for the field of crystallography when in 1982 certain materials were found [1] with diffraction patterns that were as point-like as those of crystals, but showed other symmetries that are not commensurate with lattice symmetry! So, these new substances, which were definitely not crystals in the classical sense, were quickly dubbed *quasi-crystals*, and opened a new branch of crystallography. At the same time, they brought forth a surge of new mathematics with which to model the new geometry involved.

It is to this mathematical side that we turn in this article. For beyond the many physical questions raised by these new quasicrystals, there is a bundle of mathematical questions. What do we mean by 'order', in particular by 'aperiodic order', how do we detect or quantify it, what do we mean by repetition of patterns, what are the underlying symmetry concepts involved, how can one construct well-ordered aperiodic patterns? Beyond this, as one quickly realizes, is the general question of how the new class of quasicrystals and their geometric models are to be placed between the perfect world of ideal crystals and the random world of amorphous or stochastic disorder or, in other words, how can we characterize the level of 'disorder' that we may have reached?

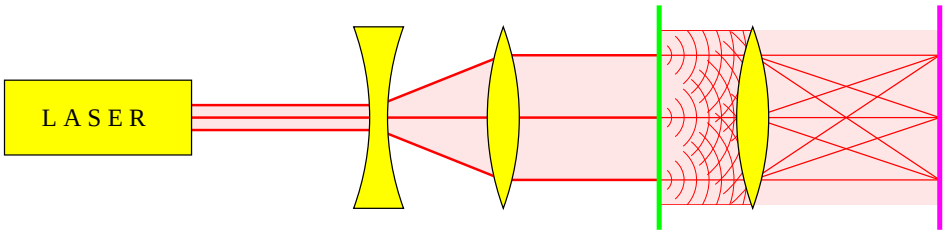

Box 1 *Experimental setup for optical diffraction*
The laser beam is widened by an arrangement of lenses and orthogonally illuminates the object located at the green plane. The light that emanates from the object plane then interferes, and the diffraction pattern is given by the distribution of light that one would observe at an infinite distance from the object. By another lens, this pattern is mapped onto the pink plane. Whereas for a picture of the object, as for instance in a camera, light rays emanating from one point of the object ideally are focused again into a single point of the picture, the situation is different in diffraction — light emanating from different regions within the object make up a single point of the diffraction pattern, as schematically indicated by the red lines in the right part of the figure. Therefore the diffraction pattern carries information about the entire illuminated part of the object. It provides some kind of measure of the correlations, and thus an account of the degree of order, in the structure of the object.

2 Planar tilings

A very instructive and also very attractive way to get a feeling for the ideas involved is to look at two-dimensional tiling models. The two rhombi (the so-called proto-tiles) shown in Box 2 are clearly capable of periodic stacking and so of lattice symmetry, the symmetry lattice being generated by the two translational shifts shown. Another possibility is shown below, which gives a tiling that is periodic in one direction and arbitrary (in particular, possibly aperiodic) in the other. On the other hand, the rhombi can also be used to tile the plane in the form of the famous Penrose tiling, see Box 3.

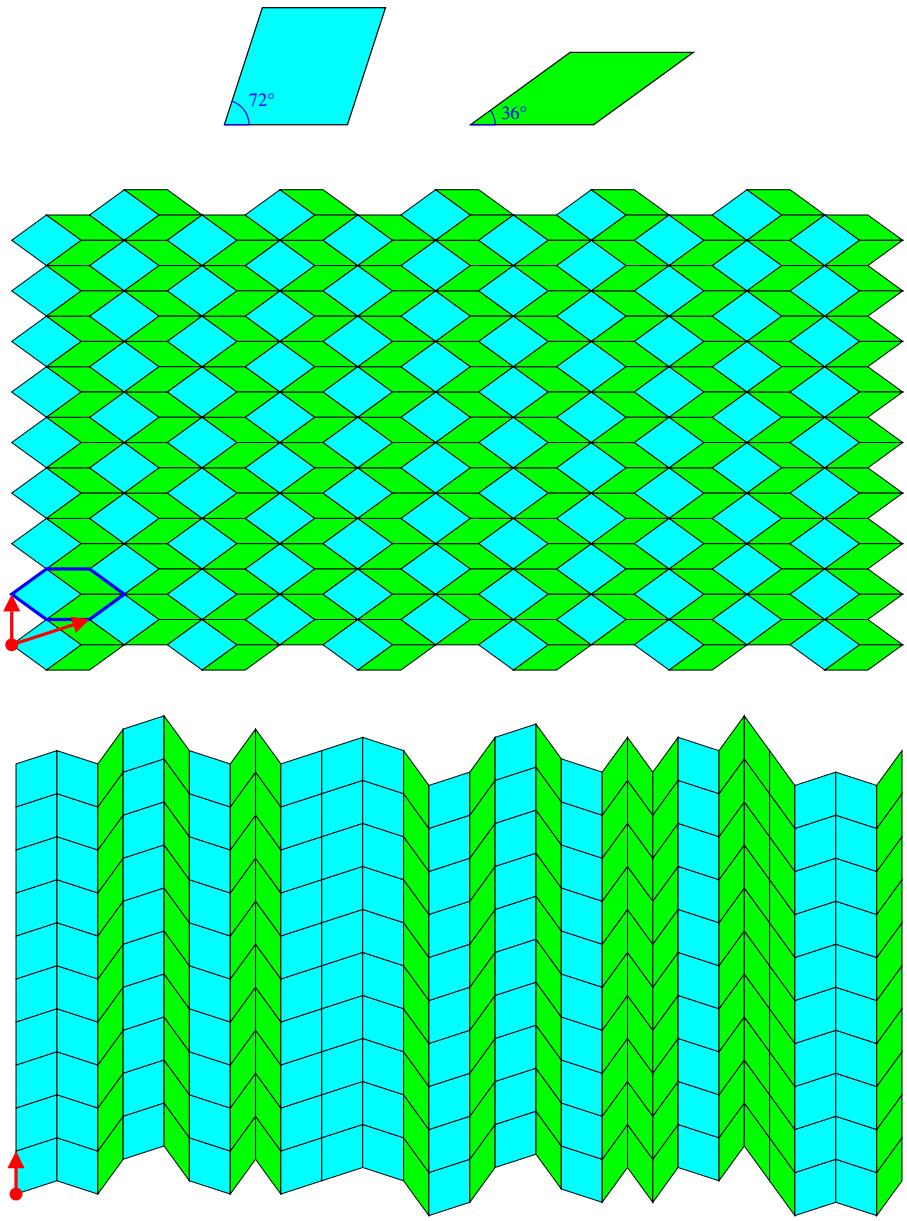

Box 2 *The undecorated Penrose tiles and some of their assemblies*
The prototiles are two rhombi, a fat one with opening angle 72° and a skinny one with 36°. They admit periodic arrangements like the one shown in the middle. The fundamental periods are indicated by arrows, and a fundamental domain in form of a hexagon is highlighted. It contains one fat and two skinny rhombi. Below, another arrangement is shown, which is periodic in the vertical direction, but admits an arbitrary 'worm' of rhombi in the horizontal direction.

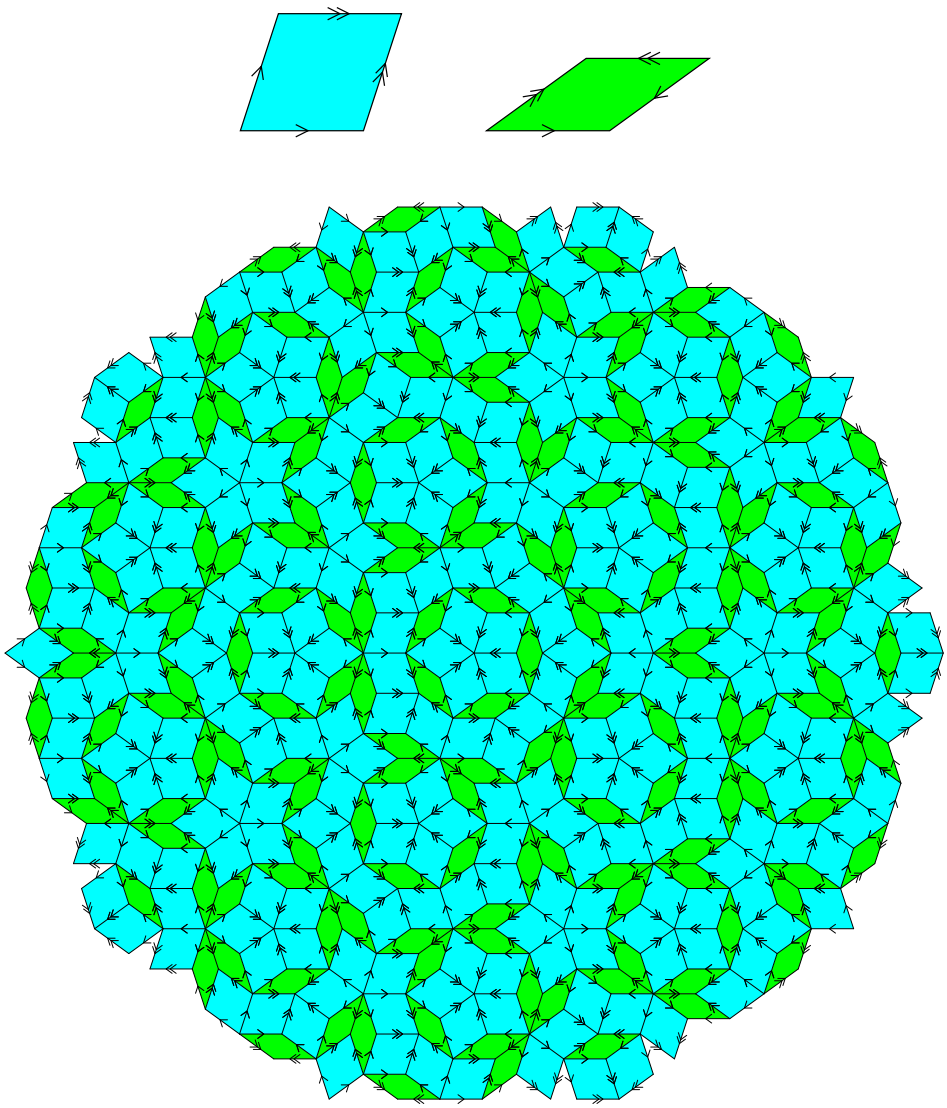

Box 3 *A central patch of Penrose's aperiodic tiling*
The two rhombi of Box 2 received a decoration of their edges by single and double arrows. If one now requires a perfect matching of all arrows on adjacent edges, the possible arrangements are highly restricted. In fact, the only permissible tilings of the entire plane are the so-called Penrose tilings. The different (global) possibilities cannot be distinguished by any local inspection. A fivefold symmetric patch of such a tiling is shown above.

Part of the intriguing nature of the Penrose tiling, of which just a circular fragment is shown in Box 3, is the obvious question of what exactly the rules might be for assembling these tiles. A properly constructed Penrose tiling has several marvellous properties of which the two most important at this point are:

- A complete Penrose tiling of the plane is strictly *aperiodic* (in the sense of being totally without translational symmetries). Our particular example shows striking five-fold symmetry.

- If we ignore the tiles and just look at their vertices instead (we might think of the resulting point set as a toy model of an atomic layer) then, remarkably, this set of points is itself pure point diffractive, i.e. in the optical bench of Box 1, it produces a diffraction image on the screen with sharp spots only.

In Box 4, we see another aperiodic tiling, this time made out of two very simple tile types, a square (which we actually dissect into two isosceles triangles) and a rhombus. Its set of vertex points shows the same type of diffraction image as the Penrose tiling, namely sharp spots only, this time with eightfold symmetry (Box 5). In Box 6, we see the beautiful idea that is the secret behind many of the most interesting tilings (including the Penrose tiles): the idea of inflating and subdividing. To apply the idea here, we directly work with triangle and rhombus.

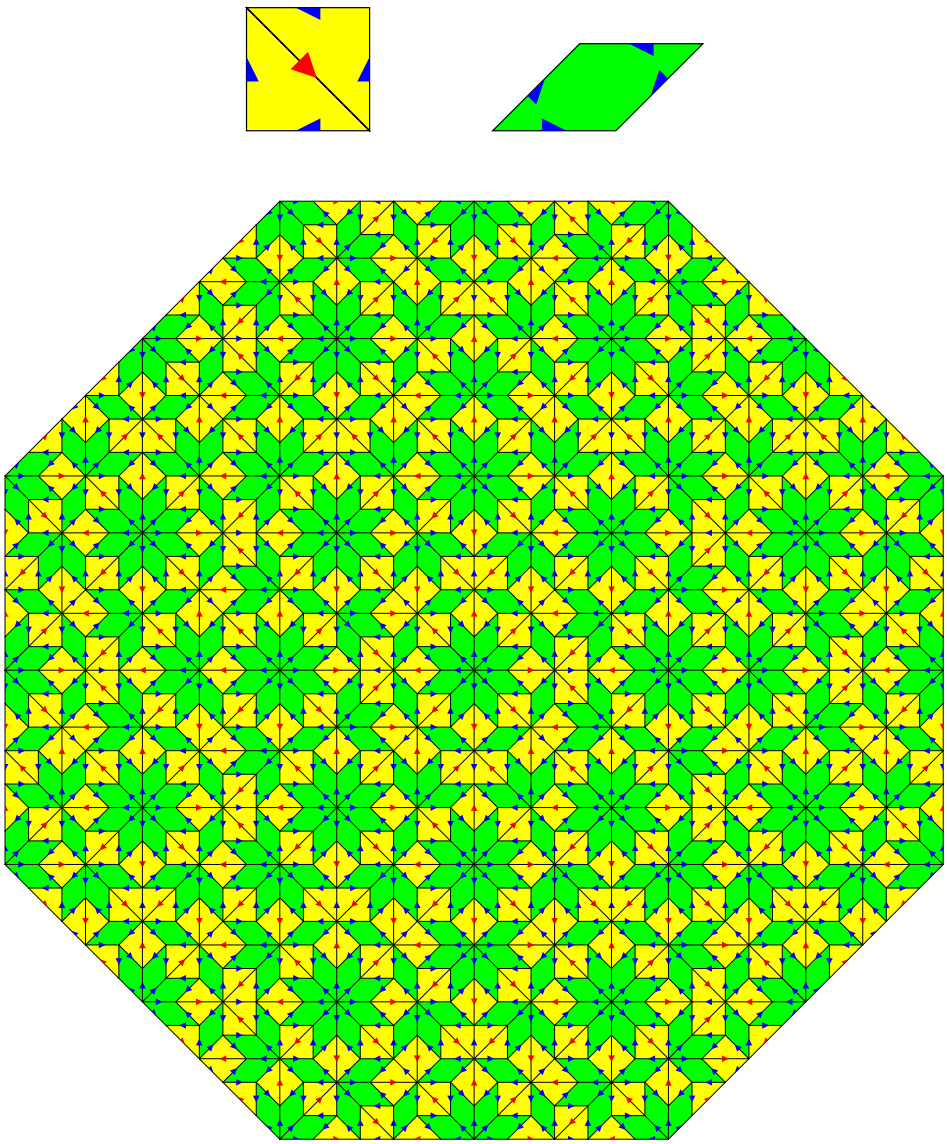

Box 4 *A central patch of the octagonal Ammann-Beenker tiling*
The original prototiles are a square and a 45° rhombus, decorated with blue arrows on the edges. For later use, the square is cut into two congruent isosceles triangles, carrying a red arrow on their common base. The orientation of arrows within each triangle is circular. Unlike the situation in the Penrose tiling, even with these arrows periodic tilings are still possible, for instance by repeating the square periodically. The octagonal patch shown belongs to the eightfold symmetric relative of the Penrose tiling, which is non-periodic and usually called the octagonal or the Ammann-Beenker tiling.

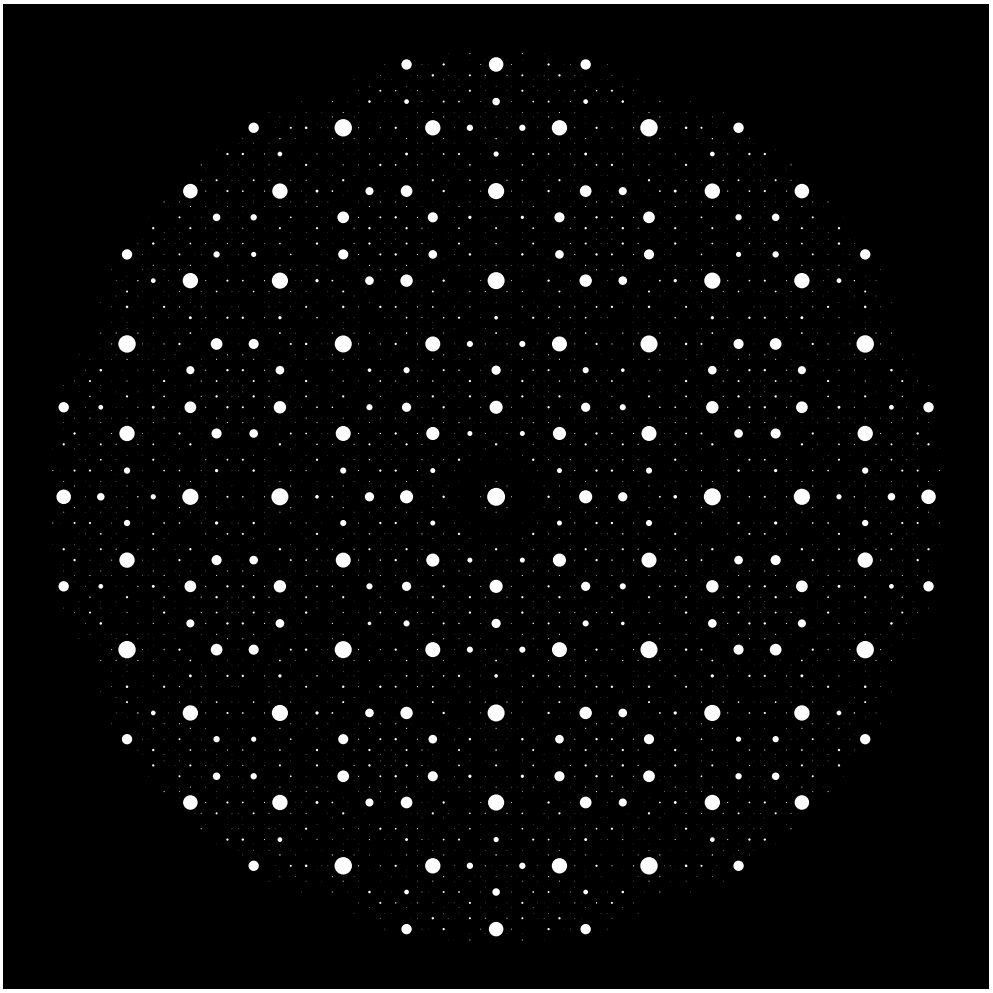

Box 5 *Diffraction pattern*
Diffraction pattern of the octagonal Ammann-Beenker tiling. The diffraction spots are indicated by circles whose area is proportional to the intensity of the diffraction peak. Spots with an intensity of less than 0.05% of the intensity of the central spot have been discarded.

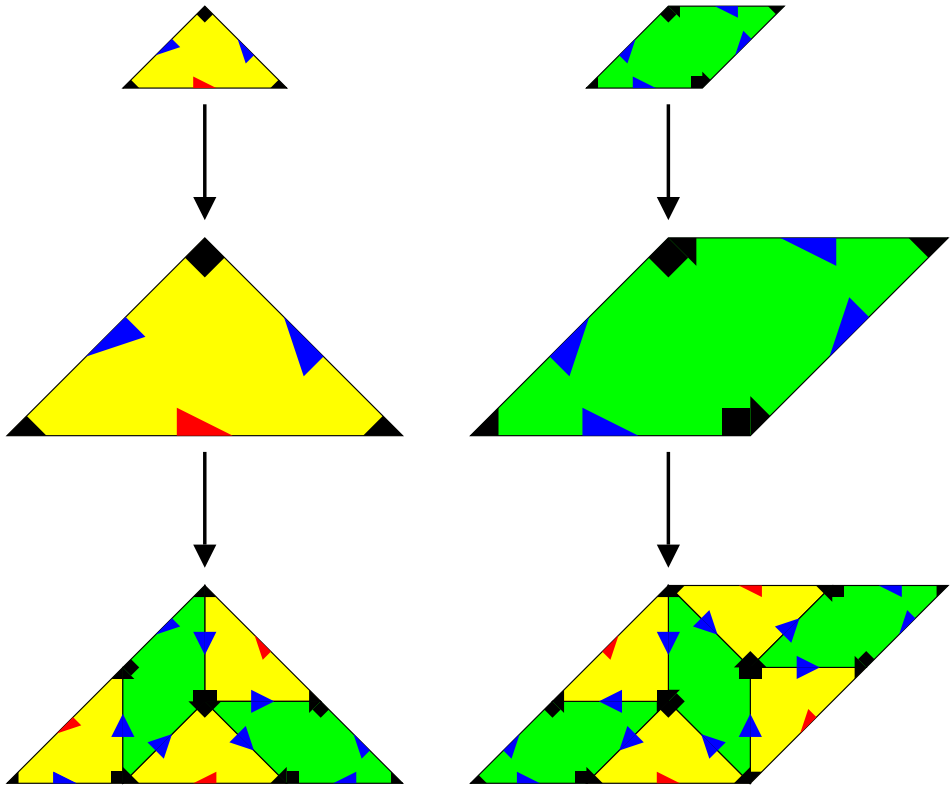

Box 6 *Inflation rule for the octagonal Ammann-Beenker tiling*
The inflation procedure consists of two steps, a rescaling by a factor of $\alpha = 1 + \sqrt{2}$, followed by a dissection into tiles of the original size. In comparison to Box 4, corner markings have been added which break the reflection symmetry of the rhombus. The patch shown in Box 4 can be obtained by applying this inflation rule (ignoring the corner markings) to an initial patch that coincides with the central octagon, filled by eight squares and sixteen rhombi. The corner markings are vital for obtaining matching rules. A sequence of inflation steps starting from a single square is shown in Box 7. Unlike the edge markings, and hence unlike the situation of the Penrose tiling, the corner markings cannot be reconstructed by local inspection of the undecorated tiling.

The inflation scheme in Box 6 shows us how to inflate each tile by a factor of $\alpha = 1 + \sqrt{2}$ and then how to decompose the resulting tile into triangles and rhombi of the original size. With this new device, we have a way of filling the whole plane with tiles. In comparison to Box 4, we added some markers in the corners of the tiles which will play some magic tricks for us later. Starting from a single tile, or from the combination of two triangles, and inflating repeatedly, we build up the sequence as shown in Box 7. Since there is no need to stop, we may go on and do this forever.

It is now easy to see that the resulting octagonal tiling has an amazing property: whatever finite pattern of tiles we see, that same pattern will be repeated infinitely often, in fact we can even specify the maximum distance we will have to search to find it again! A pattern with such a property is called repetitive. A perfect crystal is an example of a repetitive structure, of course, but the inflation procedure produces interesting new cases.

How does this happen? Imagine the partial tiling obtained after n inflations of an original patch P that consists of two triangles which build a square. It is composed of triangle pairs and rhombi. If we choose from it a patch P' which is a copy of P, then n steps after this patch was created, another patch P'' will show up which is a copy of P'. Furthermore, the position and orientation of P'' relative to P' will be the same as that of P' relative to the original P. Thus the pattern P, or a similar copy thereof, is bound to appear over and over again. In our example, P is just made of two tiles, but this idea works for any patch P that occurs somewhere in the inflation process, no matter how big it is.

The reason behind this is that the square, centred at the origin, is the seed of a fixed point under even numbers of inflation, as can be seen from the sequence in Box 7. The term 'fixed point' means that the sequence tends towards a global covering of the plane which is then left invariant (hence fixed) by further pairwise inflation steps, i.e., we have reached a stable pattern this way.

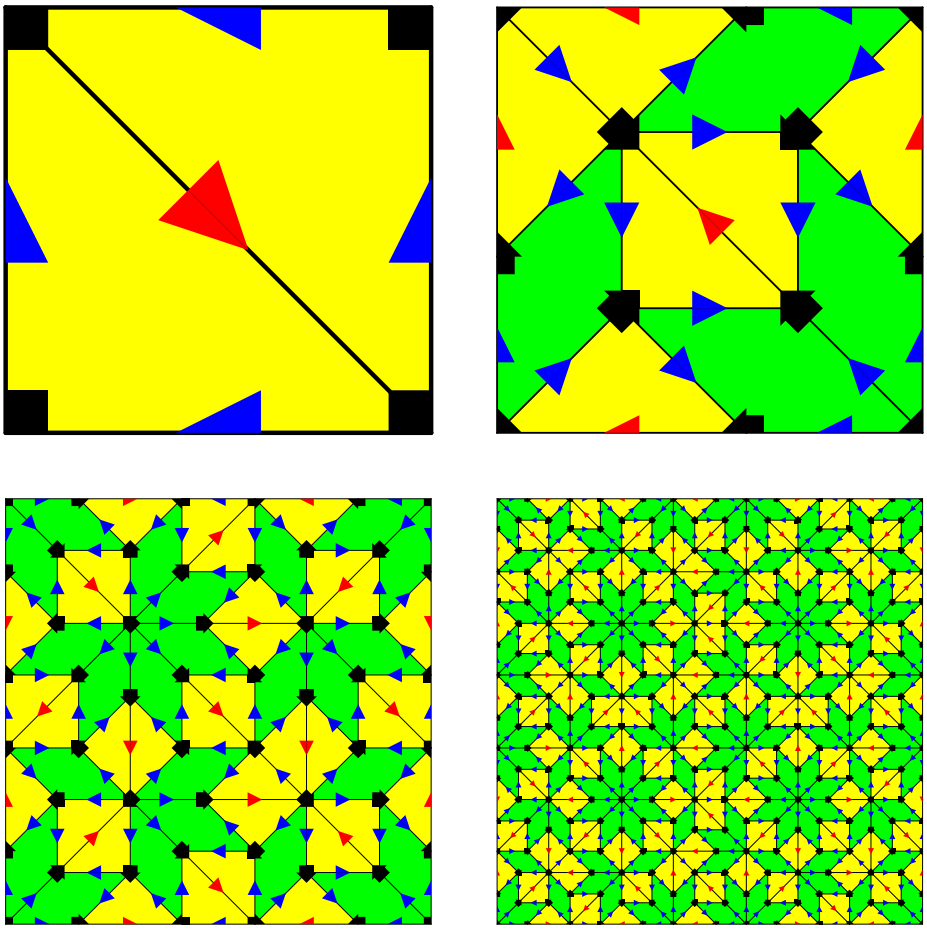

Box 7 *Repeated inflation steps of the octagonal tiling*
The sequence shows a square as an initial patch and three successive applications of the inflation rule of Box 6. (For the sake of presentability, we ignored the proper relative scale.) The inflation rule ensures that the corner markings always assemble a complete 'house'. Alternatively, assembling patches tile by tile, all complete tilings of the plane with this property and matching arrows on all edges are locally indistinguishable from the fixed point tiling created by inflation. Thus, arrows and houses together establish perfect matching rules.

So our pattern is *repetitive*, but in fact it has no periodic component at all! This is not self-evident yet, but it will become more so later. The main point right now is that the tiling has the strange and seemingly paradoxical property of having repetitivity on all scales, no matter how large, but with no periodic repetition. All patches repeat, but not periodically!

The Penrose tilings can also be built through substitution and likewise are repetitive without periodic repetition, see [2]. Thus they too have the striking property that you cannot really know where you are in the tiling by looking at any finite region around you. It follows that it is not possible to build such a tiling by any finite set of rules which tell you what to do next by looking at some finite neighbourhood of your position! To see why, imagine that this were possible. Then every time the same pattern appeared, the rules for continuing from it would be the same as those used for building at its previous occurrence. The result is that the pattern would globally repeat.

Having said this, the next reaction is going to be that our next assertion says the opposite. In fact there are assignments of marks — so-called matching rules — to the edges of the Penrose rhombi (Box 3), or to the edges and corners of the Ammann-Beenker tiles (Boxes 6 and 7), such that, if they are match everywhere in the tiling, the result is a perfect Penrose or a perfect Ammann-Beenker tiling, respectively. What is the catch?

The problem is that these matching rules guarantee that what you are getting is a Penrose tiling *as long as you never get stuck*. The trouble is that to not get stuck requires knowledge of the entire tiling to that point — it is not derivable from local information only!

3 Cut and project sets

In view of these difficulties, one might ask what other possibilities exist to systematically create arbitrarily large faultless patches of these tilings. The idea of what is going on is more easily understood by first considering an even simpler object, namely a one-dimensional inflation tiling. This time we begin with two tiles

which we call B (for blue) and R (for red), respectively. We give the short tile B the length 1 and the long tile R the length $\alpha = 1 + \sqrt{2}$ (the same number also appears in the octagonal tiling). Inflation is stretching by a factor of α, followed by a subdivision which is consistent with $\alpha \cdot 1 = \alpha$ and $\alpha \cdot \alpha = 2\alpha + 1$. The final

result is

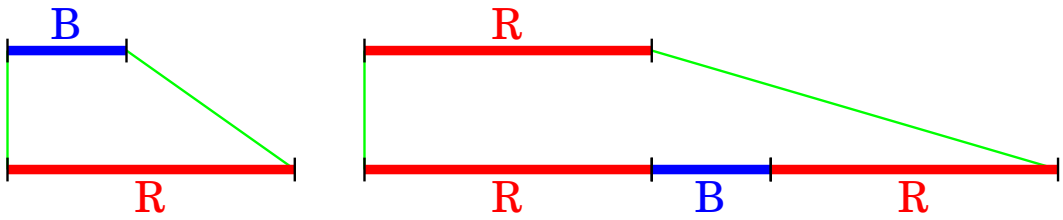

Starting from a pair of R-tiles, centred at the origin, we have successively

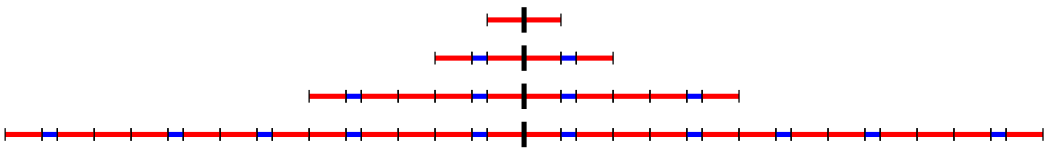

Using coordinates to label the left end point of each tile we have

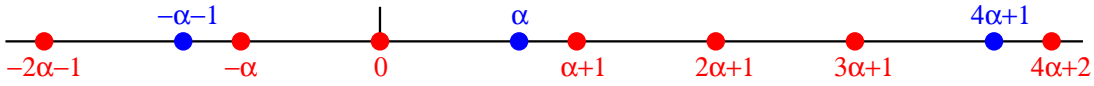

The corresponding points form an infinite set $A = \{\ldots - \alpha - 1, -\alpha, 0, \alpha, \alpha + 1, 2\alpha + 1, \ldots\}$.

What is striking about the points of A is that they are all of the form $u+v\sqrt{2}$. How can we see which points $u + v\sqrt{2}$ are present and which not? Everyone knows that it is a good idea in dealing with square roots to see what happens if you change the sign of the square root. (Think of the high school exercises in rationalizing expressions of the form $\frac{1}{1+\sqrt{2}}$.)

Let us use this trick of replacing each appearance of $\sqrt{2}$ by its conjugate, $-\sqrt{2}$. This conjugation is called the star map, the image of a point $x = u + v\sqrt{2}$ is $x^* = u - v\sqrt{2}$. Box 8 shows a plot of our points. We make a new picture in which each point x is "lifted" to the point (x, x^*) in the plane. Our points of interest are shown against a backdrop consisting of all possible points $(u + v\sqrt{2}, u - v\sqrt{2})$ where u, v are integers.

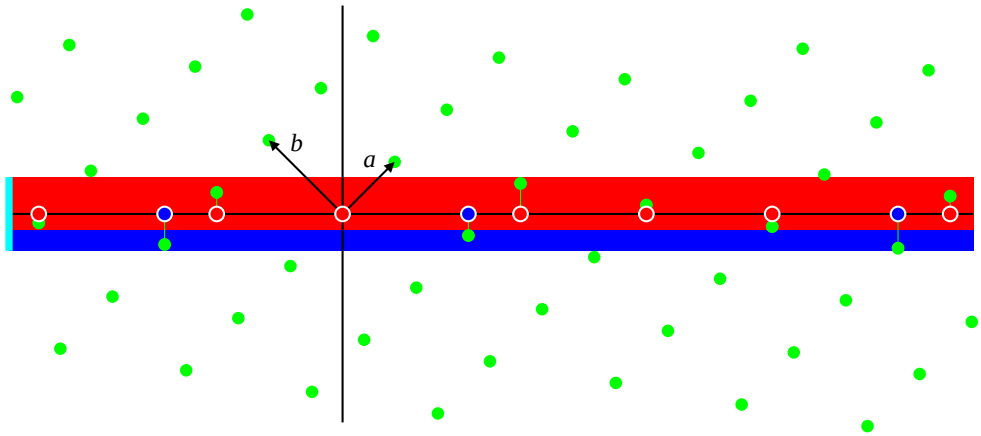

Box 8 *An alternative way to construct the point set A*
The green points form the lattice $\{(u+v\sqrt{2}, u-v\sqrt{2}) \mid u, v \text{ integer}\}$ which is spanned by the basis vectors a and b. The orientation of the strip is irrational with respect to the lattice, i.e., the black line at its centre hits the origin, but no further lattice point. The green points within the strip are orthogonally projected onto the horizontal black line and are coloured according to their vertical position in the strip. The resulting set of red and blue points coincides with the point set constructed above by inflation.

The effect is striking. The entire set of points, including the backdrop, produces a lattice (a mathematical crystal). The B and R points now appear in a band that runs from height $-\frac{1}{\sqrt{2}}$ to $\frac{1}{\sqrt{2}}$. Furthermore, the B points come from the bottom portion of the band, from $-\frac{1}{\sqrt{2}}$ to $\frac{1}{\sqrt{2}} - 1$, and the R points from the remaining top portion of the band. The actual points labelling our tiling, i.e. the set A, can be obtained just by dropping the second coordinate of each lattice point that lies in the band — in other words by projecting it onto the horizontal axis.

Now one sees that it is incredibly easy to compute the left hand end points of our 1D tiling, and hence to get hold of the tiling itself. On a computer, generate, in some ordered way, points of the type $u+v\sqrt{2}$. For each one look at its conjugate $u - v\sqrt{2}$. Test whether this number lies in either of the intervals corresponding to B and R points (e.g., $-\frac{1}{\sqrt{2}} < u - v\sqrt{2} < \frac{1}{\sqrt{2}}$ for B points) and choose the point and its colour accordingly. What we have accomplished here, apart from

the visual clarity, is a remarkable way of connecting the geometry of our tiling with an algebraic method of calculating it.

A point set that can be described in this way (by cutting through a lattice and projecting the selected points) is called, not surprisingly, a cut and project set. In this case the object that is used to cut (or to sweep out) the correct band is the vertical line segment indicated in black in Box 8. It is called the *window* of the projection method.

Another benefit of the cut and project view is that it shows immediately why the resulting point sets are aperiodic. For example, a period of our set of red and blue points is a shift t (to the left or right) that moves the set on top of itself. Necessarily it would be of the form $r + s\sqrt{2}$ since all our points have this form. However, after our lift into 2-space, we would then find that shifting by $(r + s\sqrt{2}, r - s\sqrt{2})$ takes the strip onto itself! This is impossible unless $r - s\sqrt{2} = 0$, i.e., $r = s\sqrt{2}$. However, $\sqrt{2}$ is irrational, while s, r are integers, so the only solution is $r = s = 0$, and the only period is 0.

4 The projection approach to planar tilings

The octagonal tiling, or more precisely the positions of its vertices, can also be described as a cut and project set. This goes via the projection of the points of a certain lattice in four dimensions, swept out by an octagon. We explain this in more detail.

The initial pool of points from which we select is given by the set M of all integer linear combinations $\{u_1a_1+u_2a_2+u_3a_3+u_4a_4 \mid u_1, u_2, u_3, u_4 \text{ integer}\}$ of the four unit vectors shown in left diagram of Box 9. This is a dense point set in the plane, and it is the two-dimensional analogue of the set $\{u + v\sqrt{2} \mid u, v \text{ integer}\}$ used above. Since the octagonal tiling consists of squares and rhombi (with unit edge length, say), the distance between any two vertex points is of this form, i.e. an element of M. Also the star map has an analogue, and it comes about simply by replacing the four vectors of the left diagram by those of the right diagram of Box 9; that is, $x = u_1a_1 + u_2a_2 + u_3a_3 + u_4a_4$ is mapped to $x^* = u_1a_1^* + u_2a_2^* + u_3a_3^* + u_4a_4^*$. As before, the set of pairs (x, x^*) forms a lattice, this time in four dimensions.

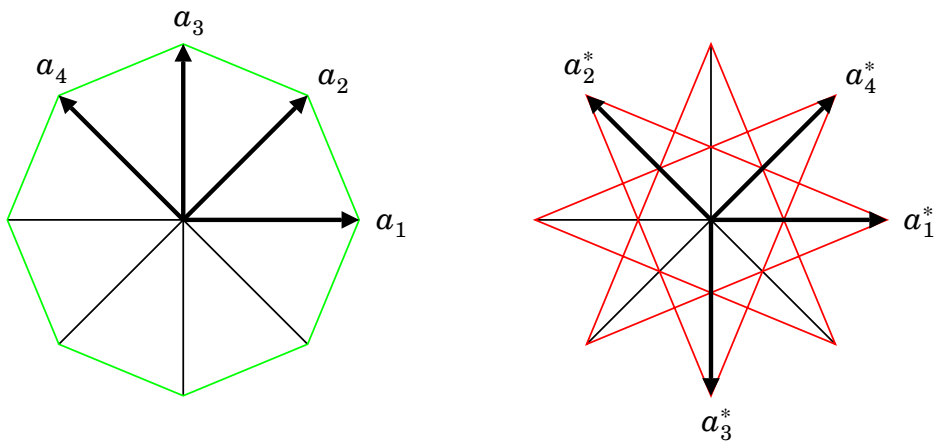

Box 9 *The two ways to count to four (and hence to eight)*
The two sets of vectors used to construct the octagonal tiling, a_i (left, for tiling space) and a_i^* (right, for internal space), $i = 1, 2, 3, 4$. The change from a_i to a_i^* demonstrates the action of the $*$-map in this case.

The vertex set of the Ammann-Beenker tiling can now be given as the set of points x whose image x^* under the star map lies inside a regular octagon of unit edge length. We can now link this back to our previous approach via inflation. If we start from a unit square and keep on inflating, as shown in Box 7, the images of the vertex points under the star map will densely populate this octagon in a uniform way, see Box 10.

Needless to say, the additional visual clarity obtained from a 4D description is debatable! Still, the conceptual idea is very powerful, providing the essential link between geometry, algebra, and analysis that is at the heart of much of our understanding of aperiodic order.

Likewise the points of the Penrose tiling can be given a cut and project interpretation, as do many other similar pointsets. In both cases, the aperiodicity can be shown in the same way as for our one-dimensional example.

Another tiling of physical interest is built from a square and an equilateral triangle. The example shown in Box 11 can be created by a slightly more complicated inflation rule, or alternatively once again by the cut and project method. In this case, however, the corresponding window shows a new feature: it is a compact set with fractal boundary. An approximation is also shown in Box 11.

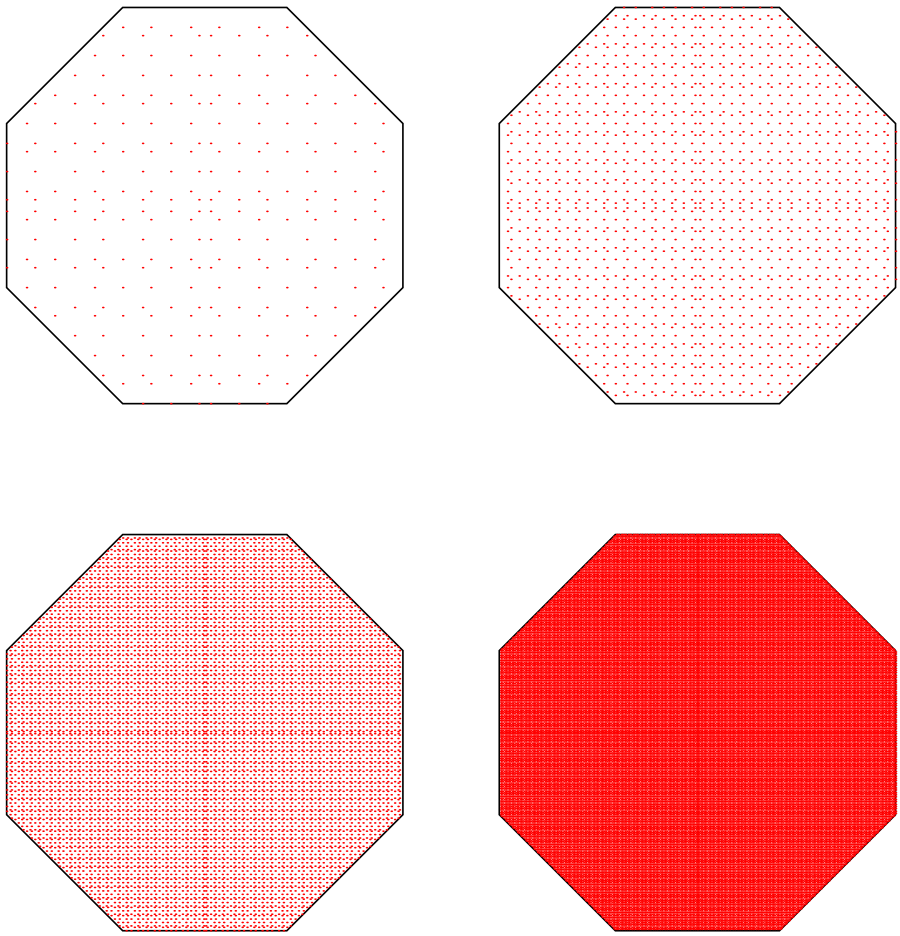

Box 10 *Filling the octagon in internal space*
The image points x^* under the star map of the vertex points are shown for larger and larger patches of the octagonal tiling, obtained by inflation of a square as shown in Box 7. Eventually, the points populate the regular octagon with uniform density. Here, the first picture of the sequence corresponds to the largest patch of Box 7.

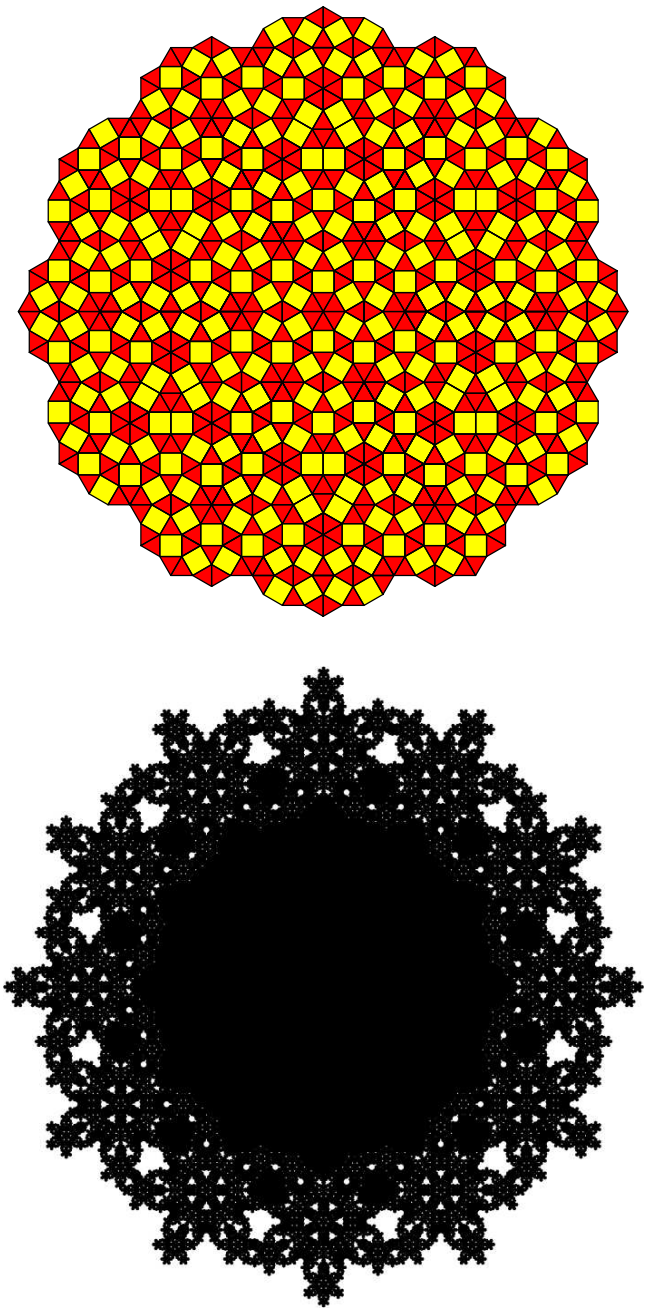

Box 11 *Quasiperiodic square triangle tiling*
This example of a square-triangle tiling can either be obtained by an inflation rule or by projection from a lattice in four dimensions. The points selected for projection lie in a generalized 'strip' whose cross section is a twelvefold symmetric object with fractal boundary.

5 The origin of diffraction

The picture that we see in Box 8 offers us considerable insight into the diffractive nature of sets that can be described as cut and project sets. The background is a lattice (crystal) and this, from the classical theory of crystals, is supposed to have perfect diffraction, i.e., the entire diffraction image is composed of sharp peaks only. The trick is how to restrict this down to the points in the band and ultimately to our line of points. Box 12 shows a picture of what happens. The bottom figure, which looks like an irregular comb, shows the diffraction of the points A of our 1D tiling. The diffraction intensity is shown here not by the size of the dots, but rather by the length of the teeth of the comb.

Above it is the diffraction picture of the background lattice, another lattice, that, as we mentioned before, is called the dual lattice. The points that carry the teeth of the comb (i.e. the spots of the diffraction) are nothing other than the projections of the points of the dual lattice — and this time *all* of them. The lengths of the teeth are provided by the profile on the right hand side. Where that profile comes from is a longer story. (Engineers may recognize its similarity to the Fourier transform of a single square pulse. It is, in fact, the square of the Fourier transform of the characteristic function of the interval defining the band.)

The teeth of the comb lie actually dense on the line. However, due to the damping nature of the profile, most of them are so small that, no matter what finite resolution we may use, we can see only a small fraction of them, and hence only an effectively discrete set of teeth, or spots, as in Box 5.

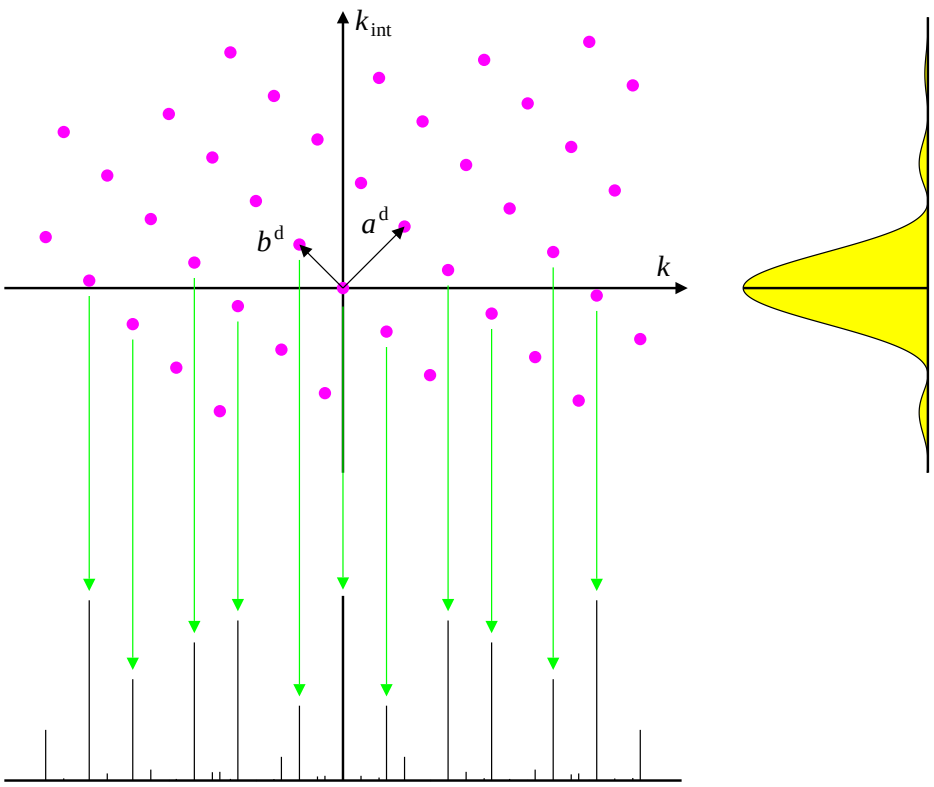

Box 12 *Explanation of the diffraction pattern*
The pink points indicate the lattice dual to the lattice of Box 8. It is explicitly given by $\{(\frac{m}{2} + \frac{n\sqrt{2}}{4}, \frac{m}{2} - \frac{n\sqrt{2}}{4}) \mid m, n \text{ integer}\}$. The lattice is spanned by the vectors a^{d} and b^{d} which satisfy the scalar product relations $a^{\text{d}} \cdot a = b^{\text{d}} \cdot b = 1$ and $a^{\text{d}} \cdot b = b^{\text{d}} \cdot a = 0$. In this case, all points of the lattice are projected, resulting in a dense set of positions on the horizontal line at the bottom. At each such position, a diffraction peak is located. Its height, i.e., the intensity seen in an experiment, is determined by the vertical coordinate k_{int} of the unique corresponding point of the dual lattice. The explicit value is given by the function $I(k_{\text{int}}) \sim \left(\frac{\sin(\sqrt{2}\pi k_{\text{int}})}{\sqrt{2}\pi k_{\text{int}}}\right)^2$ which is displayed on the right hand side.

6 What are cut and project sets?

The realization of our point sets as lingering images of lattices in higher dimensional spaces is both visually appealing and sheds light on diffraction. However, the use of conjugation as we used it appears as a miracle and one is left wondering why it worked and when we might expect it to work again. In fact, the answer to this is not really known. We do not know when a given aperiodic point set, even if it is pure point diffractive, may be realized in the cut and project formalism. We do know that they are not restricted to sets involving irrationalities like $\sqrt{2}$. One of the most interesting and earliest examples of this is the one based on the Robinson square tiles.

These tiles arose out of another one of the streams whose confluence produced the subject of aperiodic order, namely the decision problem for tilings. Given a finite number of tile types, is there an algorithm for determining whether or not the plane can be tiled (covered without gaps and overlaps) by translated copies of these tiles? This problem had been raised and later brought to a negative conclusion by logicians. Tiles that only can tile aperiodically lie at the heart of this undecidability, and the hunt was on for the smallest collections of such tiles.

Raphael Robinson made a very interesting contribution to this by first linking the problem of tiling a plane with marked square tiles to Turing machines and the famous Halting Problem, and also coming up with a simple set of 6 square tiles with markings (shown in Box 13 — actually 28 tiles since all rotated and reflected images are also to be included) that only tile aperiodically. A rather dramatic proof of this can be glimpsed from the subsequent pictures where it is seen that legal arrangements of the tiles lead to a family of interlocking squares of increasing (by factors of 2) sizes. The aperiodicity is obvious: no finite translation could take the squares of all sizes into themselves.

If we mark the centre of each tile by a coloured point (to indicate its type) then we get 6 (or 28) families of points which are subsets of a square lattice. These point sets are in fact cut and project sets, but now the 'higher dimensional' space is far more exotic: it is the product of a Euclidean plane and an arithmetical-topological space that is based on the so-called 2-adic numbers. In spite of being very different from a Euclidean space, the diffraction results are provable much as before. Each of these point sets is pure point diffractive!

There remains though, the difficult problem of characterizing cut and project sets.

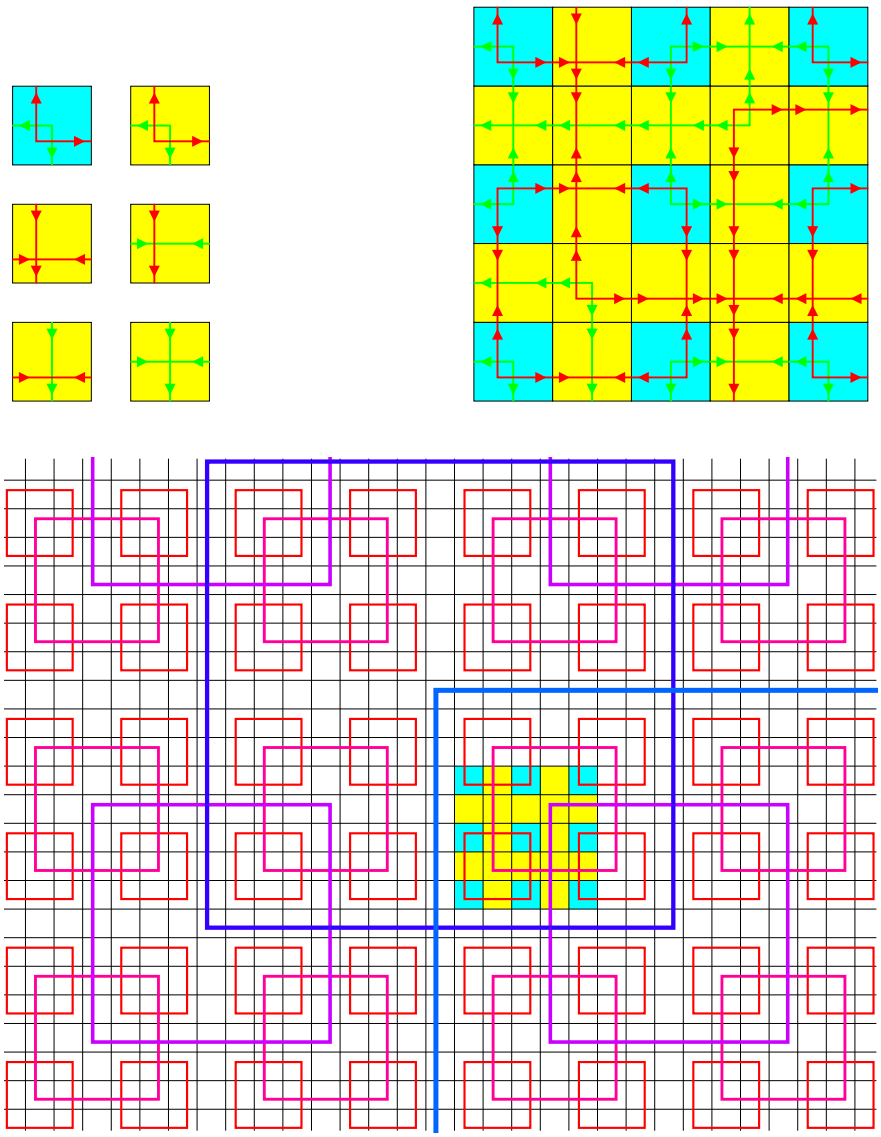

Box 13 *Robinson tiling*
The six Robinson tiles (upper left) given as squares of two different colours that are labeled by two types of oriented lines. Together with their images under rotation and reflection they make up an aperiodic set of tiles, if one requires that the oriented lines match at the edges, and that exactly three yellow squares meet at each corner (upper right). Disregarding the green lines, the red lines make up a pattern of interlocking larger and larger squares, indicated by different colours in the lower picture. The region tiled by coloured squares corresponds to the patch shown above.

7 Probabilistic ideas

As was briefly mentioned in the beginning, quasicrystals can also be seen as a stepping stone for bridging the gap between perfect crystals on the one extreme and amorphous solids on the other. It can clearly only be a first step, as we have seen how close they are to crystals in so many properties.

Indeed, as all constructions above have shown, quasicrystals are completely deterministic, and what is still missing here is a source for some kind of randomness, or stochastic disorder. This would be an entire story in itself, but we can at least indicate one way to use crystallographic and quasicrystallographic tilings to make some steps into this new direction. The new facet here is that the underlying mechanism is *statistical* in origin, both for the reason of existence and for the appearance of symmetries, which are also statistical now.

Inspecting Box 4 again, we now remove all markings, and also the long edges of the triangles. We obtain a square-rhombus tiling, with many "simpletons". By these we mean little (irregular) hexagons built from one square and two rhombi, as shown in Box 14. They can now be flipped as indicated, without affecting any face-to-face condition. If we randomly pick such simpletons and flip them, and continue doing so for a while (in fact, for eternity), we arrive at what is called the square-rhombus random tiling ensemble. A snapshot is shown in Box 15.

In this way, we have introduced an element of randomness into our tiling, but without destroying the basic building blocks (the square and the rhombus) and their face-to-face arrangements. Also, this does not change the ratio of squares to rhombi. Nevertheless, there are many such tilings now, in fact even exponentially many, i.e. the number of different patches of a given size grows exponentially with the size! This means that the ensemble even has positive entropy density, which opens the door for a completely different explanation of why we see them in nature: they are, given the building blocks (e.g. in the form of rather stable atomic clusters that can agglomerate), "very likely". Recent evidence seems to point into this direction, and a more detailed investigation of these random tilings is desirable.

In fact, one could even start from just a pool of tiles of both types and admit all assemblies that cover the plane without gaps or overlaps, and without violating the face-to-face condition of the tiles. This way, one gets an even larger class of tilings, called the unrestricted square-rhombus random tiling ensemble, where arbitrary ratios of squares to rhombi are realizable. Among them, we also find the ones constructed by randomization of perfect tilings as explained above, and one can show that the tilings of maximal entropy (which basically means the most likely ones of this enlarged ensemble) have the square-rhombi ratio of the perfect Ammann-Beenker pattern and show eightfold, hence maximal, symmetry! The latter has to be interpreted in the statistical sense, meaning that each patch one can find occurs in all 8 orientations with the same frequency. This brings about a totally different symmetry concept which is statistical rather than deterministic

in origin, a somewhat puzzling thought perhaps. Nevertheless, this is sufficient to make the corresponding diffraction image exactly eightfold symmetric!

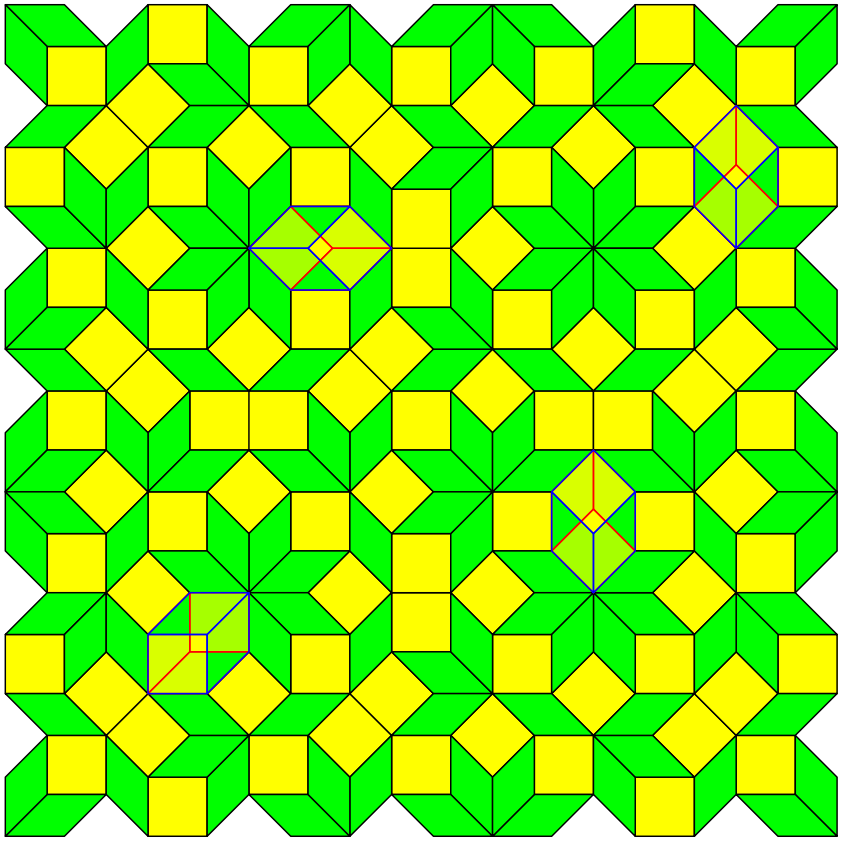

Box 14 *Simpleton flips*
Four examples of simpleton flips in a patch of the perfect Ammann-Beenker tiling. The hexagons and their original dissection into a square and two rhombi are marked by the blue lines, whereas the red lines indicate the flipped arrangement. Note that only the three internal lines in the hexagon are affected by the flip, the outer shape stays the same. One can view the patch, and all variants obtained by such elementary simpleton flips, also as the projection of a (fairly rugged) roof in 3-space — the two versions of the simpleton fillings then correspond to the projection of two different half surfaces of a cube.

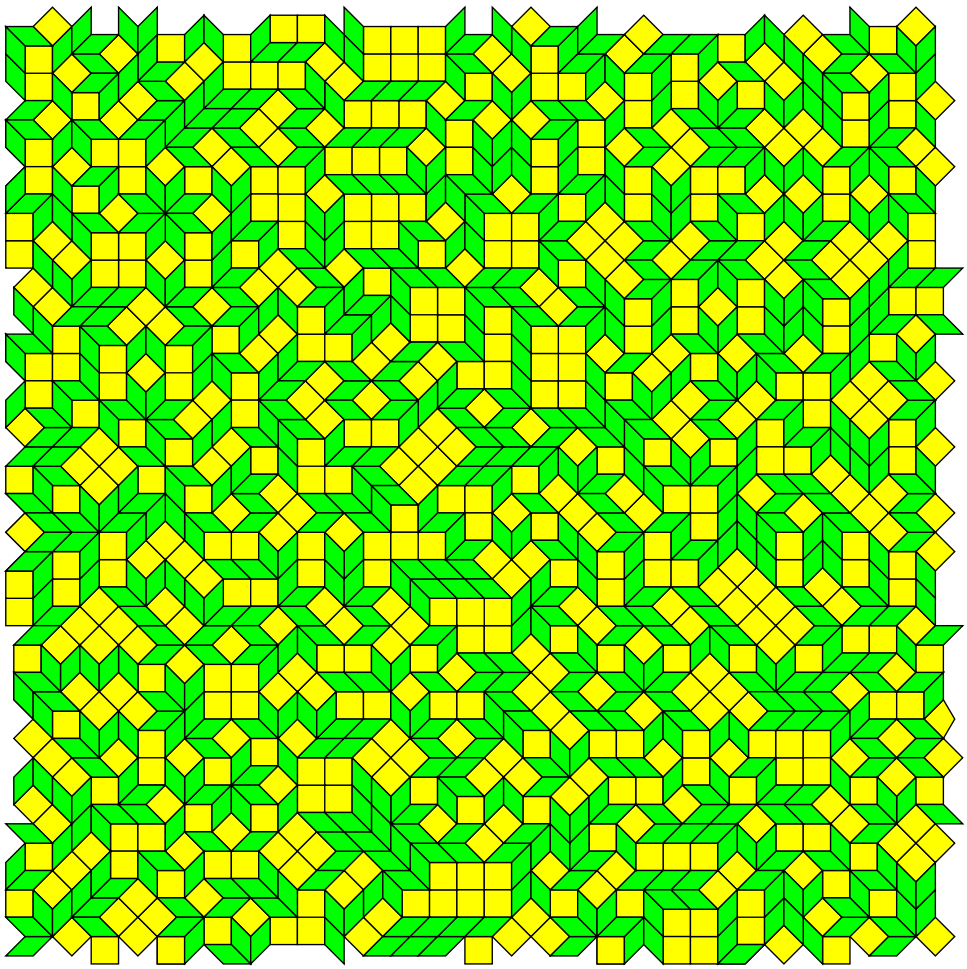

Box 15 *Square-rhombus random tiling*
A patch of a square-rhombus random tiling obtained by randomly rearranging a large approximating patch of the perfect Ammann-Beenker tiling. In fact, we started from a square-shaped patch as those shown in Box 7, whose translated copies, when glued together along its boundaries, generate a periodic pattern that violates the perfect matching rules only in the corners where the pieces are glued together. The same procedure could be applied to the disordered patch shown here, resulting in a periodic pattern which simply has an enormously large building block, namely the one shown above!

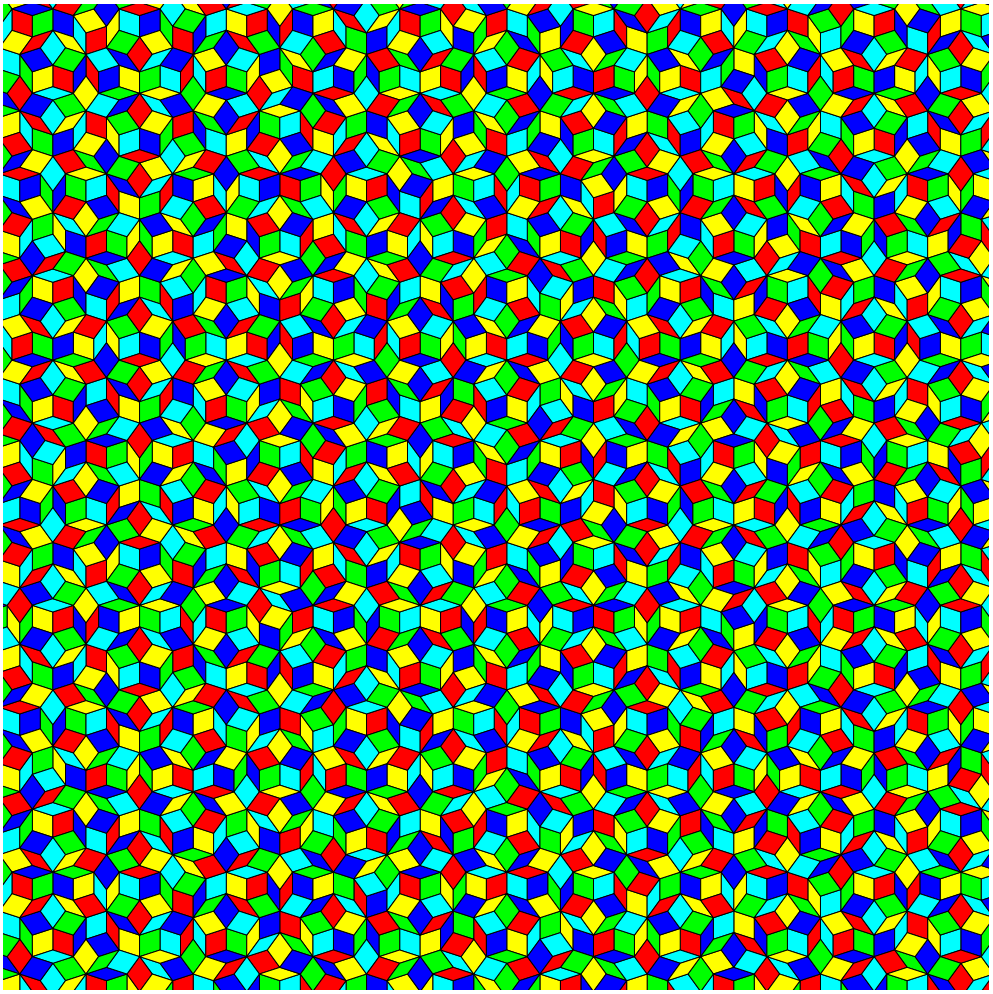

Box 16 *A colour-symmetric Penrose tiling*
The picture shows a colouring of the Penrose tiling with five different colours. The colours are chosen such that they permute in a definite way under rotation of the tiling. Figure courtesy of Max Scheffer (Chemnitz).

8 Summing up

One fascinating thing about the type of order exemplified in this discussion is how very close it comes to being periodic without admitting any actual periods.

So, let us ask again: 'what is aperiodic order?'. At present, we have a reasonable qualitative and a partial quantitative understanding, some aspects of which we have tried to explain above. However, we still don't have a complete answer, and such an answer might lie well into the future.

But what we do know is that there is a universe of beautiful questions out there, with unexpected results to be found, and with many cross-connections between seemingly disjoint disciplines. On top of that, it is definitely a lot of fun, for example, when producing new variants of Penrose tilings with colour symmetries, such as the example shown in Box 16 below! For a recent bibliographical review of the literature, we refer the reader to [4].

References

[1] D. Shechtman, I. Blech, D. Gratias, and J. W. Cahn, *Metallic phase with long-range orientational order and no translational symmetry*, Phys. Rev. Lett. **53** (1984) 1951–1953.

[2] B. Grünbaum and G. C. Shephard, *Tilings and Patterns*, W. H. Freeman, New York (1987).

[3] G. Harburn, C. A. Taylor, and T. R. Welberry, *Atlas of Optical Transforms*, Bell, London (1975).

[4] M. Baake and R. V. Moody (Eds.), *Directions in Mathematical Quasicrystals*, AMS, Providence, RI (2000).